Artificial Ground Freezing by Solid Carbon Dioxide – Analysis of Thermal Performance

Petr Nikolaev[a,b1], Majid Sedighi[a], Hamid Rajabi[a,c] and Alexander Pankratenko[b]

[a] Department of Mechanical, Aerospace and Civil Engineering, School of Engineering, The University of Manchester, Oxford Rd, Manchester, M13 9PL, United Kingdom

[b] Department of Construction of Underground Structures and Mines, Mining Institute, National University of Science and Technology MISIS, Leninskyi pr. 4, Moscow, 119049, Russia

[c] Department of Civil Engineering and Industrial Design School of Engineering, University of Liverpool, The Quadrangle, Brownlow Hill, L69 3GH, United Kingdom

Abstract:

Artificial ground freezing (AGF) is a ground improvement technique that is commonly used to create temporary earth support and groundwater control system during underground constructions (tunnels, shafts and mines). In the past two decades, solid carbon dioxide (SCD) has received increasing interest as a source of cold to freeze the soils. SCD provides a faster and safer solution to lower the ground temperature below the freezing point compared with alternative and conventional AGF techniques using refrigerants such as liquid nitrogen (LN). The existing analytical models for the design of AGF cannot provide accurate prediction of the SCD-based artificial ground freezing as they do not consider the specificity of heat transfer to the sublimated SCD. In addition, they neglect the thermal resistance due to the effects of the layers of freeze pipe, drilling mud and casting materials in the overall heat transfer. We present a new semi-analytical model for the formation of a frozen body during SCD-based ground freezing that takes into account the presence of additional sources of thermal resistance at the

[1] Corresponding author: Petr Nikolaev, Petr.Nikolaev@manchester.ac.uk

freeze pipe. The proposed model describes the formation dynamics of single-ice cylinders and plane ice-wall along with temperature distributions within the freezing mass and SCD consumption. The proposed model is tested against the known laboratory test results and alternative numerical models to demonstrate the accuracy of the solution for predicting all characteristics of ice-wall dynamics.

Keywords: Artificial ground freezing; Ground improvement technique; Solid carbon dioxide; Two-phase Stephan problem; Tunnelling.

1. Introduction

Artificial ground freezing (AGF) is a temporary construction technique to provide safe excavation, improving slope stability and groundwater control in mining and underground construction projects (Andersland et al., 2004; Bell, 2013; Harris, 1995; Trupak, 1974). AGF has been proved to be a reversible eco-friendly process to temporarily convert the soil moisture into ice in order to improve the hydro-mechanical properties of the ground. Soil particles in the artificial freezing process are firmly consolidated by the locally formed iced particles, creating an ice wall with higher strength and lower permeability compared to the unfrozen soil. There are generally two types of coolants used in AGF: i) liquid brine (calcium chloride) which is circulated in chilled conditions (-25 to -35 ^{o}C) throughout a closed network of buried freeze pipes and surface refrigeration system (Andersland et al., 2004), and ii) expandable refrigerants, e.g. liquid nitrogen (LN), which is poured into open freeze pipes, where it is vaporised at a low temperature (down to -196 ℃) (Harris, 1995). Interest in the use of solid carbon dioxide (SCD) in the ground freezing projects has recently emerged with a number of successful demonstration applications; particularly in Russia (Nikolaev and Shuplik, 2019a; Shuplik and Nikolaev, 2019; Shuplik, 1989). This method assumes direct loading of the granulated SCD into freeze pipes, where it sublimates and reduces the temperature of the freeze pipe wall to the sublimation temperature (down to -78.9 ^{o}C). The use of SCD in ground freezing provides a simpler and safer coolant compared with LN (Shuplik and Nikolaev, 2019).

Accurate prediction of the thermal behaviour of the ground freezing process by SCD sublimation is critical for the design and implementation, especially to achieve a complete formation of ice walls and a secure excavation/workspace. Thermal analysis is specifically critical for the evaluation of the freezing front location, design of piping arrangement plan, freezing time and the optimisation of the refrigerant consumption for a cost-effective ground freezing design.

The foundation of the method that is currently used to design the SCD freezing works was created by Shuplik (1989). Accordingly, for typical geological conditions, the parameters can be defined based on empirical relationships that were obtained from a set of laboratory experimental studies. However, for the wide range of geological conditions, the empirical method may not provide an accurate prediction of the frozen wall delivery (Nikolaev, 2016).

Due to the complexity of the AGF problem and the absence of analytical solutions, the main approach for the AGF design is numerical simulations (Alzoubi et al., 2020). However, this approach is usually time-consuming for studying the scenarios for engineering optimization which is a critical step in the AGF design. Moreover, SCD ground freezing is often used in emergencies when the ground freezing parameters must rapidly be determined. The analytical solution can be also effectively used to specify the thermophysical properties of soils during the freezing by comparing the sets of analytical results with the measured temperature fields.

It should be noted that the known analytical and semi-analytical models of the AGF cannot accurately combine heat flow and groundwater migration (Alzoubi et al., 2020). However, in ordinary geological conditions, the velocity of groundwater rarely exceeds 2 m/day. This value does not affect the process of ice wall formation by the brine freezing method (Andersland et al., 2004), therefore, it also does not prevent the creation of ice wall by SCD ground freezing. Due to that, in the present paper, the effects of groundwater flow on the ice wall formation are not considered.

This paper, for the first time, presents a semi-analytical model for the design of single-ice cylinders and a plane-ice wall in AGF (i) that considers real-time dynamics of ice-wall formation by the SCD ground freezing method to define freezing time, the temperature distribution within ice-wall and refrigerant consumption and (ii) that includes the effects of thermal properties of freeze pipe materials, drilling mud and casting pipes in ground freezing. The ice walls are assumed to be shaped through two stages during ground freezing which include the formations of single ice cylinders and a united ice-wall as a flat plane body (Lunardini and Varotta, 1981; Trupak, 1974). If the diameter of the ice-wall that is being created by a single freeze pipe is larger than the distances between the neighbouring pipes, the ice-wall may be considered a flat plane body (Cai et al., 2019, 2018). In both stages, it is assumed that unsteady-state analytical and semi-analytical solutions to the heat transfer problem can independently be developed. Semi-analytical and analytical solutions for a thin ice-wall are usually derived from single-ice cylinder formation theory mostly for Neumann boundary conditions applied to freeze pipe's wall (Boles and Ozisik, 1983; Li et al., 2018; Zhou et al., 2018). The existing solutions proposed for the heat transfer problem in ground freezing are not suitable for SCD assisted-freezing since the associated boundary condition for the case of SCD assisted-freezing is rather a Dirichlet boundary condition (i.e. constant temperature on the inner freeze pipe's surface). It has been reported from laboratory studies (Nikolaev, 2016; Shuplik, 1989) that the grains of SCD are attached to the freeze pipe's wall and maintain its temperature around -70-74 ^{o}C during the whole freezing process.

Only a few analytical/semi-analytical solutions to the formation of a single ice cylinder that consider Dirichlet conditions have been proposed. Cai et al. (2018) proposed a generalisation of the solutions by Jiang et al. (2010) and Zhou and Zhou (2012). However, due to the assumptions that were made during its construction the perfect accuracy compared to the numerical solution was not reached. This solution was complemented by the semi-analytical relations for the flat plane body formation in (Cai et al., 2019). Another approach was formulated by Xu et al. (2020), however, due to the nonlinearity in the proposed two-phase Stefan approach, its application to the engineering practice may be limited. In addition, there is an absence of an analytical capability to assess the distributions of temperature within a thick ice-wall created by single or multi-row freezing pipes (Alzoubi et al., 2020). The accurate solutions for the temperature distribution in circular and linear ice-walls (with constant surface temperature) are only available for the steady-state heat transfer (Hu et al., 2019; Shao et al., 2020).

These models usually divide soil around a freeze pipe into frozen and unfrozen zones. In real operations, the diameter of freeze pipes is lower than that of boreholes due to the necessity of space for installation simplicity (Davydov, 1980), and the freeze pipe after installation is covered by a thick layer of drilling mud and, possibly, one or several layers of casing pipes. The application of the polymeric freeze pipes was recently proposed to use in excavations by tunnel boring machines (TBMs) to avoid damage to their cutting tools after AGF completion (Cai et al., 2020). The thermal resistance of polymeric pipes and heat conductivity of casing and mud layers might be different from surrounding soil and should be considered in AGF design (Shuplik and Nikitushkin, 2011). Plastic freeze pipes with better isolation are also suitable for long-term freezing projects to control energy loss, where they can be an alternative to the air-insulated freeze pipes discussed by (Zueter et al., 2020, 2021). In this case, the thickness of the plastic pipe can be adjusted for the thermal resistance of the freeze pipe needed in a different geological profile.

Available field data are limited for AGF by solid carbon dioxide (Nikolaev, 2016; Shuplik and Nikolaev, 2019), and do not include complete sets of the necessary description of the geological conditions, thermo-physical properties and/or loading condition of SCD. Therefore, to assess the accuracy of the developed model, ,we compare the computational results with the datasets of a unique laboratory experiment by Shuplik (1989), another semi-analytical model (Cai et al., 2019, 2018) and with numerical simulation.

The paper is structured as followed. In Section 2 we briefly discuss the idea of the SCD ground freezing method and the experience of its application. In Section 3 we derived the semi-analytical solution for the formation of a single ice cylinder and a line flat ice body that take into account the presence of additional sources of thermal resistance at the freeze pipe surface, such as the materials of freeze and casting pipes walls and the drilling mud layers. In this section, we also proposed the relationships for the expandable refrigerant consumption rate. In Sections 4 – 7 we considered several test problems and compare the results of the developed semi-analytical solutions with the numerical results that were obtained by the finite element method (FEM) simulation. The main conclusions are drawn in Section 8.

2. Artificial ground freezing by solid carbon dioxide

2.1 Overview of the method

The simplest way of using granulated SCD for ground freezing is to load it directly into the freeze pipes (Nikolaev and Shuplik, 2019; Shuplik and Nikolaev, 2019), where it sublimates and withdraws heat from the surrounding soil reducing its temperature to about -78.8 ^{o}C depending on the pressure in the pipe (see Fig. 1). The ice-cylinders around freeze pipes gradually merge to form a thin ice-wall with a typical height up to 40 m (Shuplik, 1989). However, some critical excavations require thicker ice walls which can be achieved by several rows of freeze pipes. Other possible schemes that use SCD as a source of cold are discussed in (Nikolaev and Shuplik, 2019; Nikolaev, 2016).

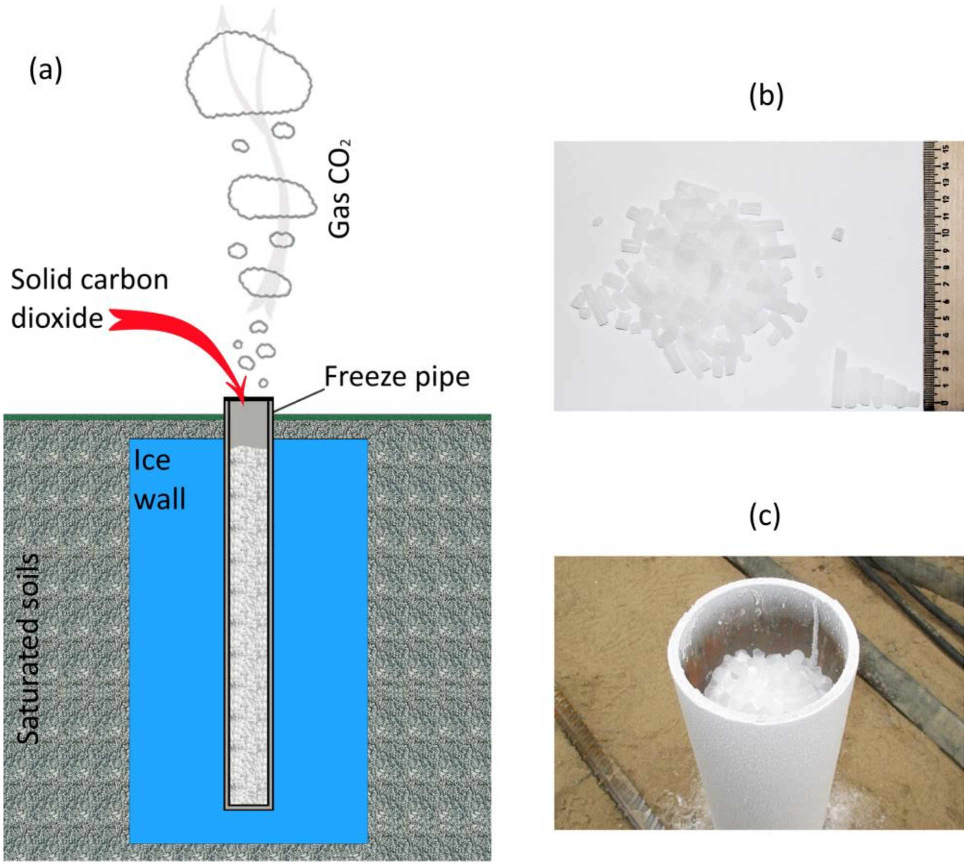

Fig. 1. Solid carbon dioxide ground freezing method. (a) – the scheme of the method; (b) – solid carbon grains; (c) – SCD in a freeze pipe

The ice-wall formation by SCD is fast, typically taking up to one week, in comparison to traditional brine delivering an ice-wall up to several weeks or months (Harris, 1995). The preparation of the ground facility for the SCD is much simpler and quicker since there is no need to ground pipelines, special storage, transportation facilities, refrigerated vehicles and major services (water or electricity). The use of SCD is fairly safe in comparison to LN, and its total amount needed for 1m^3 of frozen soil is three times lower than LN (Nikolaev, 2016). The SCD freezing method has currently fully replaced LN freezing in Moscow underground construction. This replacement happened because of two major reasons. First, due to the more complicated installation process of the LN freezing system, the total time that is necessary to stabilize the given amount of soils for LN and SCD freezing are approximately the same. At the same time, the cost of LN freezing is much higher. The second reason is that LN freezing is a complicated and dangerous method (there are known cases when inhalation of extremely cold LN gas coming out from the freeze pipes or direct contact with the liquid by workers leads to fatal consequences), that needs special cautiousness during the workflow; at the same time, SCD freezing can be realized with little special preparations by unqualified workers.

2.2 Brief history of the method application

For the first time in civil engineering practice, the SCD was initially used in the AGF to stabilise permafrost soils in the middle of 1960th (Maksimov and Zamyatin, 1969). Nearly at the same time, the possible application of the SCD to freeze soils was mentioned by Shuster (1972), but since then it hasn't been developed worldwide. However, the application of solid carbon dioxide for freezing soils has been actively developing in the Soviet Union and later in Russia. It was used in many construction projects, some of them are discussed in (Nikolaev, 2016; Shuplik, 1989), see also (Shuplik and Nikolaev, 2019).

At the earlier stage of the method development, the typical volume of frozen soils for one project was between 300 and 1000 m^3. In the recent applications, this range has significantly increased. For example, in 2016-2018, during the construction of the connection tunnel between the newly built 'Petrovskyi park' station and the operating 'Dinamo' station of the Moscow subway system, more than 3000 m^3 of soil were frozen by SCD to ensure the safety of construction work at the depth between 25 and 40 m in fully saturated unstable soils close to the operating station and tunnels. In 2018, this method of freezing was applied to stabilize more than 2500 m^3 of soils around the cutter head of a 10.7m TBM to support the maintenance works that were conducted to replace the TBM's cutting tools that wear out untimely in unsuitable geological conditions during the construction of the 15th subway line (see Fig. 2).

It should be noted that in that project, the significant difficulties arose due to the large inclination of the freeze pipes from their project positions, which reached up to 2m, even if the freeze pipe lengths were only up to 40m. It happened because the soils around the TBM were compacted, mixed and damaged by a 10m TBM that was unsuccessfully pushed forward with blunt cutting tools. However, for normal method application, where untouched soils are frozen, the inclination of freeze pipes is quite small due to their short length (mostly up to 20m, rarely up to 40m) and the high accuracy of modern boring equipment. Because of that, the borehole inclination may be neglected during the SCD ground freezing design.

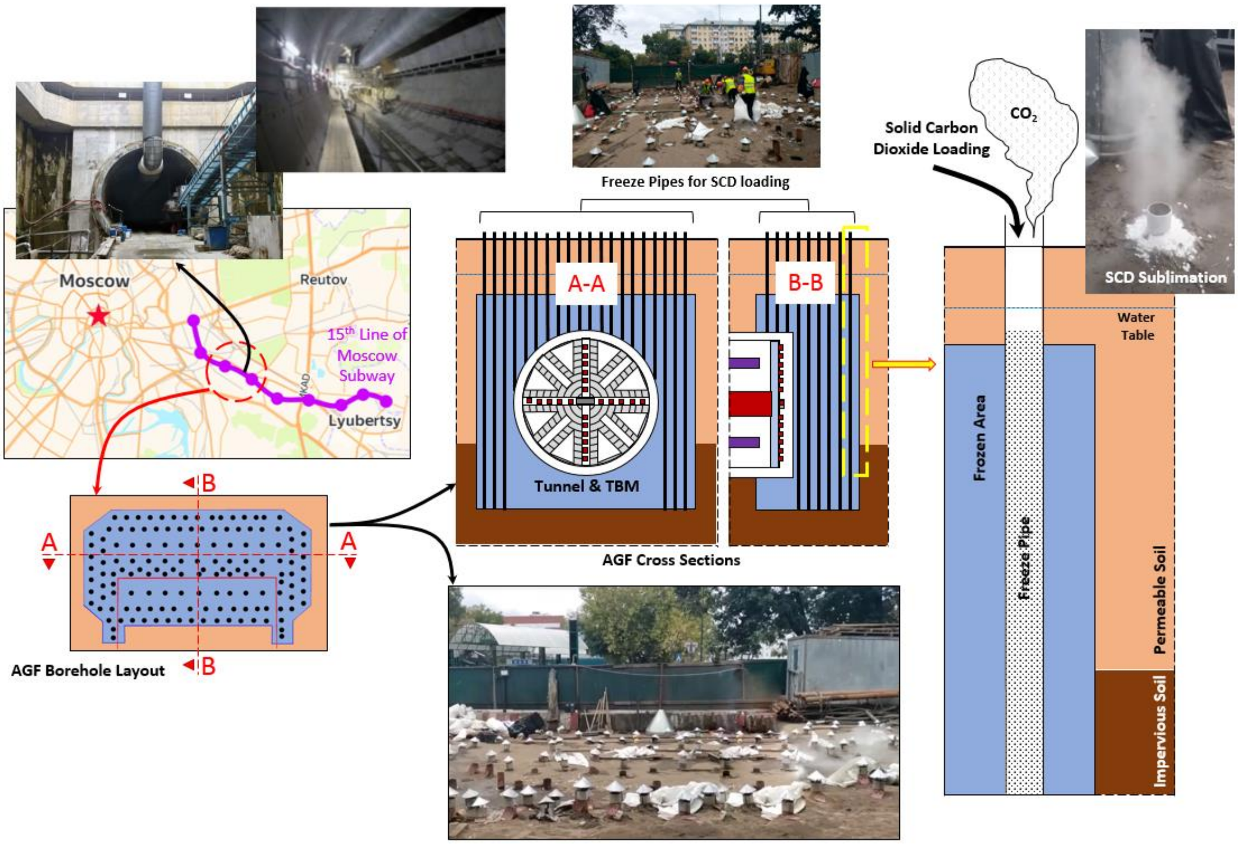

Fig. 2. Ground freezing during tunnelling of the 15th line of the Moscow subway system

In 2020, this method was used to liquidate an emergency that happened at a depth of more than 25m during the sinking of one of the construction pits for the second circle line of the Moscow subway system. In that project, the volume of soils that has been frozen by this ground improvement method has reached 3700 m^3, for which around 1500 tonnes of SCD were used. The existing experience indicates that the applied design method cannot properly predict the consumption of the SCD that very often led to the overconsumption of the refrigerant. In the current projects, the assurance coefficient that is used during the estimation of the total necessary amount of SCD can reach 1.3 - 1.5, which was fairly acceptable for small construction projects when the total necessary amount of SCD rarely exceeded a couple of hundred tons. However, for the large projects typical for nowadays practice, such a coefficient leads to a difference of more than one thousand tons between the project applied (prepaid and delivered) amount of SCD and the really necessary refrigerant total consumption. Due to that, the development of the new design method is an important and relevant engineering task.

3. Semi-analytical model of ice-wall formation

The formation process of an ice-wall by the AGF can be generally divided into two phases: (a) the formation of individual ice cylinders until they are merged together and (b) the development of a united ice-wall in the form of a flat plane body (Lunardini and Varotta, 1981; Trupak, 1974). In the present paper, we will follow this approach. Additionally, to this assumption, several others are used:

- Soil thermal properties are homogeneous and constant for both states (liquid and solid). The densities of ice and water are equal; therefore, the coupled mechanical effect is neglected.
- No groundwater flow is presented in freezing soils, i.e. natural and forced convection is ignored;
- The entire volume of groundwater is frozen at the same constant temperature which makes it possible to neglect the presence of a transition (mushy) zone between liquid and frozen regions. The thermodynamic equilibrium is established immediately after the phase change.
- As the SCD ground freezing is mainly used to freeze the soils between 10 and 40 m depths, where the temperature of soils is nearly constant, temperature in the developed

model is assumed to be independent to depth. Therefore, the problem is reduced to 1D heat transfer.

- The phase change of water within the drilling mud layer is not considered. At time $t = 0$, the layer with $n = k$ already exists with a small thickness.
- Temperature of the inner surface of the freeze pipe is constant during the entire freezing period.
- There is a uniform initial temperature of the soil layer. The temperature at the infinite distance from the freeze pipe is constant.

3.1. Formation of a single ice cylinder

The freezing of soils around a single freeze pipe can be represented in the following way. The temperature field around a single freeze pipe in a two-dimensional domain can be assumed to be a sum of $k + 1$ cylindrical layers, that represent the exact location of the freeze pipe wall, drilling mud and casing pipe wall, see Fig. 3. As shown in this figure, R_0 as inner radius of a freeze pipe wall and R_n is the outer radius of n^{th} layer. The layer of frozen soil has $n = k$ and $R_k = R_k(t)$, and the layer of unfrozen soil has $R_{k+1} = \infty$. Here, n and k are positive integer numbers. A cylindrical coordinate system is applied to describe the heat transfer process.

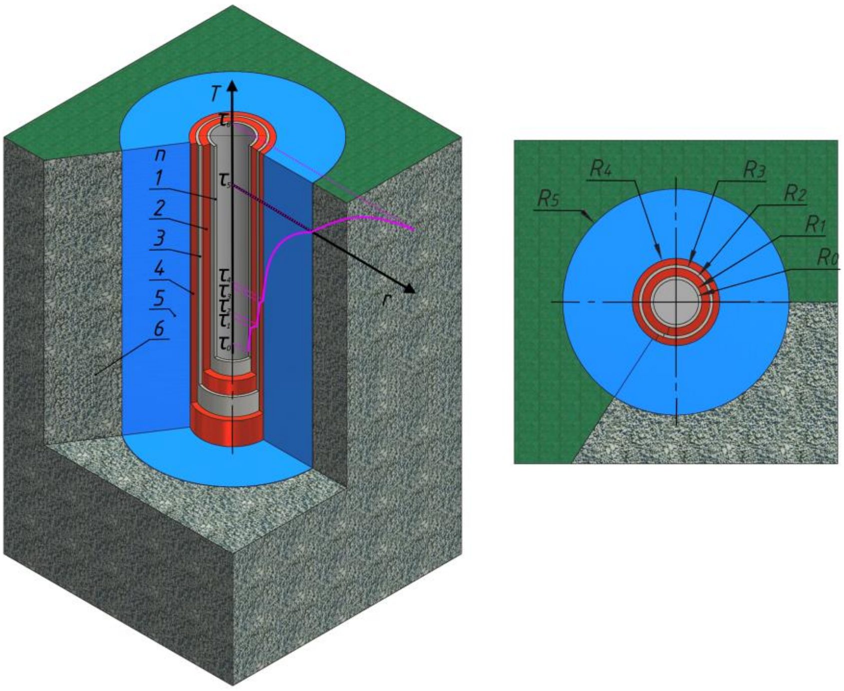

Fig. 3. The geometry of the proposed analytical model of a single ice cylinder consisting of freeze pipe wall (n = 1), drilling mud layer (n = 2), casting pipe wall (n = 3), drilling mud layer (n = 4), frozen soils (n = 5) and an unlimited layer of unfrozen soils (n = 6).

The partial differential equation for heat conduction in a cylindrical coordinate system for the n^{th} layer is (Kakaç et al., 2018):

$$\frac{\partial T_n}{\partial t} = \alpha_n \left(\frac{\partial^2 T_n}{\partial r^2} + \frac{1}{r} \frac{\partial T_n}{\partial r} \right), \quad R_{n-1} \leq r \leq R_n \tag{1}$$

where $T_n = f(r, t)$ is the temperature distribution within the n^{th} layer, t is time, $\alpha_n = \frac{\lambda_n}{(c_n \rho_n)}$ is a thermal diffusivity coefficient of materials within n^{th} layer. λ_n [W·(m·°C)$^{-1}$], c_n [J·(kg·°C)$^{-1}$] and ρ_n[kg/m^3] are thermal conductivity, heat capacity, and density, respectively. In order to develop the solution to Eq. (1), the initial and boundary conditions for the temperature that are related to the change of the temperature in the radial direction must be defined. In the development of the model, an assumption that temperature does not vary with depth is made. Such assumption is fairly accurate, as the ground freezing by solid carbon dioxide is mainly used in the interval of depth between 10 and 40 meters, where temperature remains constant during the year and does not significantly vary with depth. It gives

- The initial temperature is equal for the layers:

$$T_n(r,0) = \tau_k\,, \qquad for\;\; n \le k \tag{2}$$

$$T_n(r,0) = \tau_{k+1}, \qquad for\;\; n = k+1$$

- At the boundaries of the layers, Dirichlet boundary conditions are considered as:

$$T_n(R_0,t) = \tau_0\,, \qquad for\;\; n = 1 \tag{3}$$

$$T_n(R_n,t) = T_{n+1}(R_n,t) = \tau_n\,, \qquad for\;\; n \le k$$

$$T_n(\infty,t) = \tau_{k+1}, \qquad for\;\; n = k+1$$

- At the boundaries between 1 to k layers, the heat flux continuity is assumed:

$$\left(\lambda_n \frac{\partial T_n}{\partial r} - \lambda_{n+1}\frac{\partial T_{n+1}}{\partial r}\right)\bigg|_{r=R_n} = 0 \tag{4}$$

- At the boundary between the layer k and $k+1$, the phase change occurs for which the Eq. (4) takes a different form given as :

$$\left(\lambda_k \frac{\partial T_k}{\partial r} - \lambda_{k+1}\frac{\partial T_{k+1}}{\partial r}\right)\bigg|_{r=R_k(t)} = L\frac{dR_k(t)}{dt} \tag{5}$$

where L(J/m^3) is the latent heat of water solidification. $\tau_n = f(t)$ is the temperature on the inner surface of the n^{th} cylindrical layer. The temperature τ_k corresponds to the freezing temperature of groundwater and τ_{k+1} is the initial temperature of soils.

The accurate solution to the heat conductivity equation with a phase change (1) can be derived by replacing the two variables of r and t by a single variable x_n following (Cai et al., 2018; Kakaç et al., 2018):

$$x_n = \frac{r^2}{4\alpha_n t} \tag{6}$$

By substituting Eq. (6) into Eq. (1):

$$\frac{\partial^2 T_n}{\partial {x_n}^2} + \left(1 + \frac{1}{x_n}\right)\frac{\partial T_n}{\partial x_n} = 0 \tag{7}$$

The solution to Eq. (7) can be found as the function of $Ei(x_n)$ (Cai et al., 2018; Kakaç et al., 2018) :

$$T_n = A_n Ei'(x_n) + B_n \tag{8}$$

where A_n and B_n are unknown parameters, and $Ei'(x_n) = \int_{x_n}^{\infty}\left(\frac{e^{-p}}{p}\right)dp$ is an integral exponential function.

The classical derivation of A_n and B_n in the case of Neumann boundary conditions at the cylindrical domain has been presented in the literature, e.g., (Kakaç et al., 2018). For the case of Dirichlet boundary conditions (3) that is of interest in this study, the values of A_n and B_n can be calculated following the same approach proposed by Cai et al. (2018). Therefore, the substitution of Eq. (8) into Eq. (7) and further return substitution (6), A_n and $B_n$are defined as:

$$A_n = \frac{(\tau_{n-1} - \tau_n)}{\left[Ei'\left(x_n|_{r=R_{n-1}}\right) - Ei'\left(x_n|_{r=R_n}\right)\right]} \tag{9a}$$

$$B_n = \tau_{n-1} - A_n Ei'\left(x_n|_{r=R_{n-1}}\right) \tag{9b}$$

For the layer $+1$, we have $Ei'\left(x_n|_{r=R_{n-1}}\right) = Ei'(x_k)$ and $Ei'\left(x_n|_{r=R_n}\right) = 0$.

The substitution of Eqs. (9) into Eq. (8) can generate relationships that define temperature distribution (T_n) in the frozen zone:

- For layers 1 to k :

$$T_n = \tau_{n-1} + (\tau_n - \tau_{n-1}) \frac{\left[Ei'\left(\frac{{R_{n-1}}^2}{4\alpha_n t}\right) - Ei'\left(\frac{r^2}{4\alpha_n t}\right)\right]}{\left[Ei'\left(\frac{{R_{n-1}}^2}{4\alpha_n t}\right) - Ei'\left(\frac{{R_n}^2}{4\alpha_n t}\right)\right]}, \quad R_{n-1} \le r \le R_n \tag{10}$$

• For the layer $k+1$:

$$T_{k+1} = \tau_{k+1} + (\tau_k - \tau_{k+1}) \frac{Ei'\left(\frac{r^2}{4\alpha_{k+1} t}\right)}{Ei'\left(\frac{R_k(t)^2}{4\alpha_{k+1} t}\right)}, \quad R_k(t) \le r \le \infty \tag{11}$$

The substitution of Eq. (10) into Eq. (4) gives:

$$\tau_n = \frac{\frac{\lambda_n \tau_{n-1}\left[Ei'\left(\frac{{R_n}^2}{4\alpha_{n+1} t}\right) - Ei'\left(\frac{{R_{n+1}}^2}{4\alpha_{n+1} t}\right)\right]}{\exp\left(\frac{{R_n}^2}{4\alpha_n t}\right)} + \frac{\lambda_{n+1} \tau_{n+1}\left[Ei'\left(\frac{{R_{n-1}}^2}{4\alpha_n t}\right) - Ei'\left(\frac{{R_n}^2}{4\alpha_n t}\right)\right]}{\exp\left(\frac{{R_n}^2}{4\alpha_{n+1} t}\right)}}{\frac{\lambda_n\left[Ei'\left(\frac{{R_n}^2}{4\alpha_{n+1} t}\right) - Ei'\left(\frac{{R_{n+1}}^2}{4\alpha_{n+1} t}\right)\right]}{\exp\left(\frac{{R_n}^2}{4\alpha_n t}\right)} + \frac{\lambda_{n+1}\left[Ei'\left(\frac{{R_{n-1}}^2}{4\alpha_n t}\right) - Ei'\left(\frac{{R_n}^2}{4\alpha_n t}\right)\right]}{\exp\left(\frac{{R_n}^2}{4\alpha_{n+1} t}\right)}} \tag{12}$$

It is noted that for layer $n = k-1$ in Eq. (12), we have $R_{n+1} = R_k(t)$.

To define the radius of the interface between frozen and unfrozen soil – $R_k(t)$ - at a given time we should assume the general form of this function. Associated parameters can be defined by solving a transcendent equation found by substitution of Eq. (10) and Eq. (11) into Eq. (5). The general form of that relation that defines the dynamics of the freezing front location can be described by:

$$R_k(t) = \beta_1 t^\omega + R_{k-1}, \quad \frac{dR_k(t)}{dt} = \omega \beta_1 t^{\omega-1} \tag{13}$$

where β_1 and ω are constants.

In the classical solution of phase change heat transfer problem (1) with Neumann boundary conditions, the parameter ω is assumed to be ½ (Kakaç et al., 2018). The same value was applied by Cai et al. (2019, 2018) for the Dirichlet boundary condition (3). However, this definition does not ensure an accurate description of the dynamics of the freezing front. If is considered that both constants of (13) as unknown, then the substitution of Eq. (10) and Eq. (11) into Eq. (5) with taking Eq. (13) into account gives:

$$\lambda_k \frac{(\tau_k - \tau_{k-1}) \exp\left(-\frac{(\beta_1 t^{\omega} + R_{k-1})^2}{4\alpha_k t}\right)}{Ei'\left(\frac{{R_{k-1}}^2}{4\alpha_k t}\right) - Ei'\left(\frac{(\beta_1 t^{\omega} + R_{k-1})^2}{4\alpha_k t}\right)} + \lambda_{k+1} \frac{(\tau_k - \tau_{k+1}) \exp\left(-\frac{(\beta_1 t^{\omega} + R_{k-1})^2}{4\alpha_{k+1} t}\right)}{Ei'\left(\frac{(\beta_1 t^{\omega} + R_{k-1})^2}{4\alpha_{k+1} t}\right)} = \frac{\omega \beta_1 L}{2}\left(\beta_1 t^{2\omega-1} + R_{k-1} t^{\omega-1}\right) \tag{14}$$

Eq. (14) shows that β_1 should not generally be a constant value, otherwise, it does not satisfy Eq. (13). However, for a range of values of ω, particularly for $t >> 0$, β_1 changes very little, see Fig. 4. Therefore, we can assume that there is a constant value ω for which $\beta_1 \approx const$ at $\tau >> 0$. The value of these parameters can be numerically found via Eq. (14) by solving it at two different time instances ($t >> 0$).

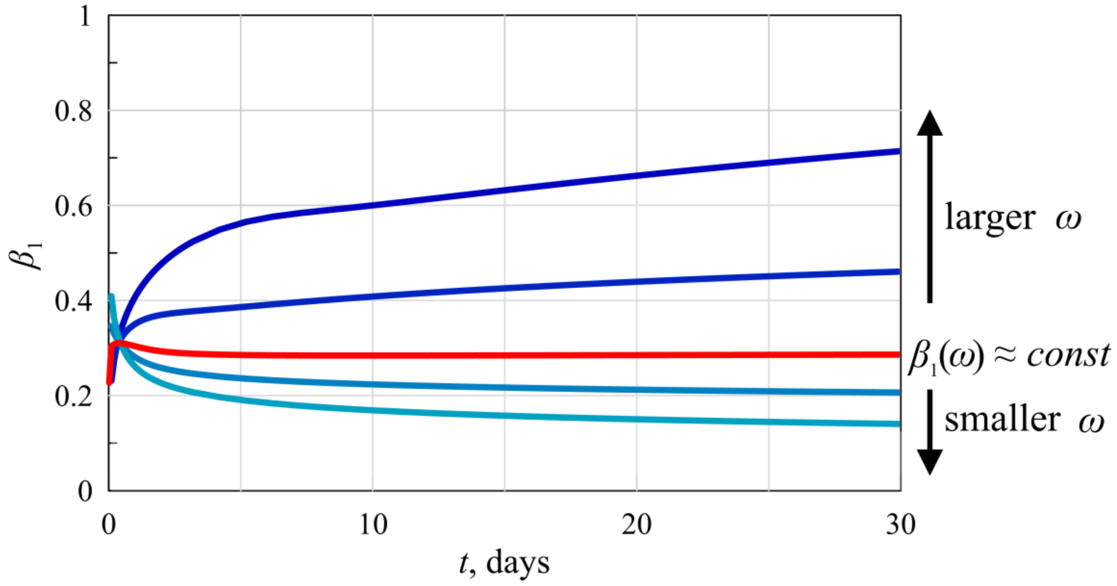

Fig. 4. Variations of function β_1 with time

Having defined ω and β_1, the formation of a single ice cylinder can be mathematically described through Eq. (13). The temperature distribution at any time and position (of the frozen front) can be found by Eq. (10) and (11).

It should be noted that a similar approach to define the dynamics of 1D soil freezing in multi-layered domains was recently independently formulated for the cartesian coordinate system by Huang and Rudolph (2022) and it was called ‘a hybrid analytical-numerical technique’.

3.2. Formation of a line ice-wall

The overlap and combination of individual ice cylinders gradually generate an ice-wall which can be described by one-dimensional solidification similar to a flat panel (Fig. 5) (Cai et al., 2019). The constant temperature of this panel should be defined as an average value in the I-I plane. The mathematical formulation of this problem is:

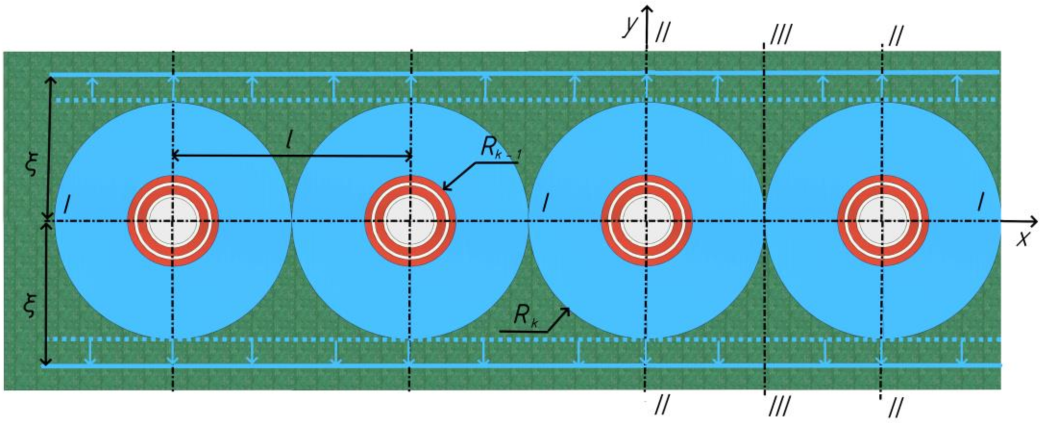

Fig. 5. Schematic of the formation of line ice-wall

$$\frac{\partial T_f}{\partial t'} = \alpha_k \frac{\partial^2 T_f}{\partial y^2}, \quad 0 \le y < \xi(t')$$
$$\frac{\partial T_{un}}{\partial t'} = \alpha_{k+1} \frac{\partial^2 T_{un}}{\partial y^2}, \quad \xi(t') \le y < \infty \tag{15}$$

with the initial and boundary conditions to be:

$$\left(\lambda_k \frac{\partial T_f}{\partial y} - \lambda_{k+1} \frac{\partial T_{un}}{\partial y}\right)\Bigg|_{y=\xi(t')} = L\frac{d\xi(t')}{dt'},$$

$$T_f(y,0) = \tau_k,\ T_{un}(y,0) = \tau_{k+1}, \tag{16}$$

$$T_f(0,t') = \widetilde{\tau_{\mathrm{I}}}, \quad T_f(\xi,t') = T_{un}(\xi,t') = \tau_k,\ T_{un}(\infty,\mathrm{t}) = \tau_{k+1},$$

where T_f and T_{un} are temperature distributions within frozen and unfrozen areas, and $\widetilde{\tau_{\mathrm{I}}}$ is the average temperature in the I-I plane for the whole period of ice-wall formation; $\xi(t')$ is the position of the phase change front. The time t' is introduced to ensure the closure of the single ice-cylinder solution of Eq. (13) to the flat panel solution at the time t_{sic}, and is defined as $t' = t - (t_{sic} - t'_{sic})$, where t'_{sic} is the time of the plane ice-wall formation with the thickness $\xi(t'_{sic}) = R_k(t_{sic})$.

The problem of 1D heat transfer with phase change, that is equivalent to the presented system of Eqs. (15) and (16), has a well-known analytical solution that is presented, e.g. in (Kakaç et al., 2018). Following to it, as a solution to the system of Eqs.(15) and (16), we can write:

- For the frozen area:

$$T_f(y,t') = \widetilde{\tau_{\mathrm{I}}} + (\tau_k - \widetilde{\tau_{\mathrm{I}}})\frac{\mathrm{erf}\left(\frac{y}{(4\alpha_k t')^{\frac{1}{2}}}\right)}{\mathrm{erf}\left(\frac{\beta_2}{(4\alpha_k)^{\frac{1}{2}}}\right)}, \quad 0 \le y \le \xi(t'), \tag{17}$$

- For the unfrozen area:

$$T_{un}(y,t') = \tau_{k+1} + (\tau_k - \tau_{k+1})\frac{\mathrm{erfc}\left(\frac{y}{(4\alpha_{k+1} t')^{\frac{1}{2}}}\right)}{\mathrm{erfc}\left(\frac{\beta_2}{(4\alpha_{k+1})^{\frac{1}{2}}}\right)}, \quad \xi(t') \le y \le \infty, \tag{18}$$

where $\mathrm{erfc}(x) = 1 - \mathrm{erf}(x)$ is a complementary error function, and β_2 is the root of the transcendent equation:

$$\frac{\lambda_k(\tau_k-\tilde{\tau}_{\mathrm{I}})\exp\left(-\frac{{\beta_2}^2}{4\alpha_k}\right)}{{\alpha_k}^{\frac{1}{2}}\mathrm{erf}\left(\frac{\beta_2}{(4\alpha_k)^{\frac{1}{2}}}\right)}+\frac{\lambda_{k+1}(\tau_k-\tau_{k+1})}{{\alpha_{k+1}}^{\frac{1}{2}}}\frac{\exp\left(-\frac{{\beta_2}^2}{4\alpha_{k+1}}\right)}{\mathrm{erfc}\left(\frac{\beta_2}{(4\alpha_{k+1})^{\frac{1}{2}}}\right)}=\frac{\beta_2}{2}L\sqrt{\pi} \tag{19}$$

where the definition of the error function is $\mathrm{erf}(x)=\frac{2}{\sqrt{\pi}}\int_0^x e^{-p^2}dp$.

The position of the freezing front is defined as:

$$\xi(t')=\beta_2 t'^{\frac{1}{2}},\quad {t'}_{sic}\leq t' \tag{20}$$

To ensure the accurate description of the considered physical problem by the proposed analytical solution (17) – (20), the temperature $\tilde{\tau}_{\mathrm{I}}$ must be accurately defined. This value must take into account the presence of additional sources of thermal resistance on the freeze pipe surface, and accurately approximate the temperature along *x*-axis and its change with the time. In (Cai et al., 2019), $\tilde{\tau}_{\mathrm{I}}$ is defined as an average of temperature of the freeze pipe wall and temperature in the middle point between the pipes when the ice-wall reaches its projected size. Here, given space average value as $\hat{\tau}_{\mathrm{I}}$, we propose a new formulation of $\tilde{\tau}_{\mathrm{I}}$ in the I-I plane that considers the presence of additional thermal resistances. It is originated from the solution for the steady-state temperature field within an ice-wall developed in (X. Hu et al., 2017; Hu et al., 2019). This solution generalizes a classical model (Bakholdin, 1963) and is based on a hydromechanical solution (Charny, 1948) as:

$$T_f(x,y)=\frac{\tilde{\tau}_{k-1}-\tau_k}{\ln\frac{2\pi R_{k-1}}{l}-\frac{\pi}{l}\xi}\left\{\frac{1}{2}\ln\left[2\left(\cosh\frac{2\pi y}{l}-\cos\frac{2\pi x}{l}\right)\right]-\frac{\pi}{l}\xi\right\}+\tau_k \tag{21}$$

where x, y are Cartesian coordinates (Fig. 5), and $\tilde{\tau}_{k-1}$ is the time average temperature of the outer surface of the multi-layered wall of the freeze pipe. To define the space average temperature of the I-I plane ($\hat{\tau}_{\mathrm{I}}$), we consider $y=0$ in Eq. (21), and then

$$T_f(x,0) = \frac{\tilde{\tau}_{k-1} - \tau_k}{\ln\frac{2\pi R_{k-1}}{l} - \frac{\pi}{l}\xi}\left[\frac{1}{2}\ln\left(2 - 2\cos\frac{2\pi x}{l}\right) - \frac{\pi}{l}\xi\right] + \tau_k \tag{22}$$

As the temperature field is symmetrical at III-III plane, we can find the integral space average value as:

$$\hat{\tau}_I = \frac{2}{l}\left[\int_0^{R_{k-1}} \tilde{\tau}_{k-1}dx + \int_{R_{k-1}}^{\frac{l}{2}} \tau_f(x,0)dx\right] \tag{23}$$

There is not an analytical solution for the second integral of Eq. (23). Therefore an approximate approach based on a Taylor series expansion has been adopted by which the logarithm in Eq. (22) at $x = 0$ gives $\ln\left(2 - 2\cos\left(\frac{2\pi x}{l}\right)\right) = 2\ln\left(\frac{2\pi x}{l}\right) - \frac{\pi^2 x^2}{3l^2} + O(x^4)$ which can be substituted into Eq. (23). If the ${R_{k-1}}^3$ is ignored, we obtain:

$$\hat{\tau}_I = \tau_k + (\tilde{\tau}_{k-1} - \tau_k)\left\{\frac{2R_{k-1}}{l} + \frac{\ln\pi - 1 + \frac{2R_{k-1}}{l}\left[1 - \ln\left(\frac{2\pi R_{k-1}}{l}\right)\right] - \frac{\pi^2}{72} - \frac{\pi\xi}{l}\left(1 - \frac{2R_{k-1}}{l}\right)}{\ln\frac{2\pi R_{k-1}}{l} - \frac{\pi}{l}\xi}\right\} \tag{24}$$

To define $\tilde{\tau}_{k-1}$, the steady-state heat flux through the multi-layered cylindrical wall is assumed which gives:

$$\tilde{\tau}_{k-1} = \tau_0 - \frac{q_w}{\pi}\left(\sum_{p=1}^{p=k-1}\frac{1}{2\lambda_p}\ln\frac{R_n}{R_{n-1}}\right) \tag{25}$$

In Eq. (25), the heat flux through the multi-layered cylindrical wall of the freeze pipe (q_w) should be known. To calculate it, we can use the classical steady-state solution (Bakholdin, 1963):

$$q_w = 2\lambda_k \tilde{\tau}_{k-1} \left(\frac{1}{\pi} \ln \frac{l}{2\pi R_{k-1}} + \frac{\xi}{l} \right)^{-1} \tag{26}$$

Substituting Eq. (26) into Eq. (25), after mathematical transformations, gives:

$$\tilde{\tau}_{k-1} = \tau_0 \left[1 + 2\lambda_k \left(\sum_{p=1}^{p=k-1} \frac{1}{2\lambda_p} \ln \frac{R_n}{R_{n-1}} \right) \Big/ \left(\ln \frac{l}{2\pi R_{k-1}} + \frac{\pi \xi}{l} \right) \right]^{-1} \tag{27}$$

The time average value of space average temperature in the I-I plane is finally defined as:

$$\widetilde{\tau_{\mathrm{I}}} = \frac{\widehat{\tau_{\mathrm{I}}}\left(\frac{l}{2}\right) + \widehat{\tau_{\mathrm{I}}}(\xi_p)}{2} \tag{28}$$

where ξ_p is the project (final) thickness of the ice-wall.

The temperature distribution within the freeze pipe wall, casting pipe walls and drilling mud layers can be defined based on the known temperature of these layer boundaries that are described by:

$$\widetilde{\tau_n} = \tau_0 - \frac{q_w}{\pi} \left(\sum_{p=1}^{p=n} \frac{1}{2\lambda_p} \ln \frac{R_p}{R_{p-1}} \right) \tag{29}$$

Eq. (20) enables us to define the dynamics of a line ice-wall formation considering drilling mud and freeze pipe wall materials. The temperature field within the multi-layered freeze pipe wall can be presented based on Eq. (29) and at any point within the frozen body by Eq. (21) and unfrozen region by Eq. (18).

3.3. Refrigerant consumption

The rate of SCD consumption within a freeze pipe - G(kg/s) - is defined based on the energy conservation law where the heat flux through the ground has to be equal to the heat flux being sorbed by the refrigerant due to evaporation or sublimation (Nikolaev, 2016; Shuplik, 1989). The consumption rates are defined as

- For a single ice-cylinder formation:

$$G_{sic} = \left(-\lambda_1 \frac{\partial T_1}{\partial r}\bigg|_{r=R_0} 2\pi R_0 h\right) \Big/ L_{CO_2} \tag{30}$$

- For a plane ice wall:

$$G_{liw} = \left(-\lambda_k \frac{\partial T_f}{\partial y}\bigg|_{y=0} 2lh\right) \Big/ L_{CO_2} \tag{31}$$

where L_{CO_2} is the latent heat of solid carbon dioxide sublimation as 572 kJ/kg.

The substitution of Eq. (10) into Eq. (30) determines the refrigerant consumption of a single ice-cylinder formation:

$$G_{sic} = \frac{-4\pi\lambda_1(\tau_0 - \tau_1)e^{-\frac{R_0{}^2}{4\alpha_1 t}}h}{L_{CO_2}\left[Ei'\left(\frac{R_0{}^2}{4\alpha_1 t}\right) - Ei'\left(\frac{R_1{}^2}{4\alpha_1 t}\right)\right]}. \tag{32}$$

The consumption for the formation of one segment of plane ice wall can be similarly predicted by substitution of Eq. (17) into Eq. (31) with taking (20) into account as:

$$G_{liw} = -\frac{2\lambda_k lh(\tau_k - \widetilde{\tau_{\mathrm{I}}})}{L_{CO_2}(\pi\alpha_k t')^{\frac{1}{2}}\mathrm{erf}\left(\frac{\beta_2}{(4\alpha_k)^{\frac{1}{2}}}\right)} \tag{33}$$

The developed semi-analytical model can be calculated in the following way.

1. The initial conditions and the model geometry is defined.
2. The parameters ω and β_1 are obtained by considering two time instances t, e.g. 3 days and 50 days.
3. A complete set of equations are established that contains two transcendent Eq. (14) for two values of t and $k-1$ Eqs. (12) which define the temperature at the boundaries between the layers τ_n. As an example, if there is no additional layer of thermal

resistance on the freeze pipe surface, there is no Eq. (12), if there is one layer, there is one additional Eq. (12).

4. This system of equations, described in step 3, is solved by a Newton-Raphson method (or similar numerical solvers).
5. When the coefficients ω and β_1 and all values of τ_n are defined, the dynamics of the ice-cylinder formation can be estimated by Eq. (13) and temperature within the layer by Eqs. (10) and (11).
6. When the radios of the single ice cylinder reach the value $l/2$, the first stage of the ice-wall creation is finished, and the plane ice-wall dynamics should be considered, which follows below steps:
7. The average temperature of the plane-ice wall boundary $\widetilde{\tau_{\mathrm{I}}}$ is defined by Eq. (28). For that Eqs. (27) and (24) are subsequently solved for $\xi = l/2$ and $\xi = \xi_p$.
8. The transcendent equation (19) is solved to find the coefficient β_2, that let us predict the dynamics of ice-wall formation by Eq. (20).
9. The temperature distribution for the unfrozen zone is calculated by Eq. (18) and for the frozen zone by Eq. (21).

In the next sections, we aim to present a set of verifications and validations of the proposed analytical solution AGF process to demonstrate its ability to describe the process of ground freezing by solid carbon dioxide. The calculation results are compared with the results of another analytical model (Cai et al., 2019, 2018). That model was chosen for the comparison as it was developed for the same set of initial and boundary conditions and the model geometry. As that model includes some assumptions, we also provide the results of the FEM numerical simulation of the same problems and the results of laboratory experiments. As there are no analytical models and experiments that consider the additional sources of thermal resistance on the freeze pipe surface, the developed model is compared with the FEM numerical simulation.

In Section 4 we will consider the solid carbon ground freezing that is modelled without taking into account the presence of additional sources of thermal resistance (free pipe wall, the layer of the drilling mud etc.). In Section 5 we validate our result by comparing the calculation results with the laboratory experiment data by Shuplik (1989). In Section 6, we will solve the case of solid carbon dioxide ground freezing to compare the possible effects of the material of freeze pipe onto the phase front dynamics. In section 7, we will discuss the ability of the model to determine the solid carbon dioxide consumption rate.

4. Verification of the semi-analytical model application to the SCD ground freezing design

This section compares the results of the analytical model and the alternative FEM solution alongside the results of the known analytical solution (Cai et al., 2019, 2018). The numerical simulation was carried out by using COMSOL Multiphysics program. The application of COMSOL for heat transfer problems with phase changes during ground freezing has also been examined and reported (Hu et al., 2018; Hu and Liu, 2016; Huang et al., 2018; Nikolaev et al., 2022; Tounsi et al., 2019). The FEM solves the partial differential equations of 1D axisymmetric and 2D heat transfer with phase changes in an isotropic homogenous medium. It should be noted, that COMSOL Multiphysics implement the apparent heat capacity method to ensure the continuous change of the thermophysical properties of soils from its frozen to unfrozen values. It leads to appearance of the transition (mushy) zone, that is neglected by the proposed semi-analytical model. However, as the applied temperature range of the transition zone (2 ^{o}C) is small compared to the freezing temperature (up to -70 ^{o}C), the presence of such region can be neglected.

Table 1. Thermal and physical properties of the soil (Case 1)

Material		Density (kg/m^3)	Thermal conductivity (W/(m^{o}C))	Heat capacity (J/(kg ^{o}C))	Latent heat of solidification ($\cdot 10^8$J/m^3)
Soft clay	Frozen	1670	2.06	1720	1.22

Unfrozen	1.65	3400

The case study deals with the formation of an ice-wall without additional cylindrical layers on the freeze pipe wall. The temperature of freeze pipe is assumed to be $\tau_0 = -70$ °C as a typical condition for SCD AGF. The inner radius of the freeze pipe is $R_0 = 0.05$ m. The soil is a soft clay with 30.3 wt.% moisture (J. Hu et al., 2017). Thermal and physical properties are provided in Table 1. It is noted that in this study the phase transition temperature is considered to be -1 ^{o}C, and the initial temperature of soils to be 10 ^{o}C.

4.1 The formation of a single ice cylinder:

The first step in the application of our semi-analytical model for the formation of a single ice cylinder is to determine the coefficients ω and β_1 (Eq. (14)). It is evident that there is a value of ω at which the parameter β_1 is nearly constant for $t > 3$ days. The function of $\beta_1 = f(\omega, t)$ is considered at two time moments of $t = 3$ days and $t = 50$ days to be able to assume $\omega = 0.422$ and $\beta_1 = 0.208$ in this problem. The position of freezing front (Eq. (13)) and temperature distribution (Eq. (10) and (11)) from the analytical solution, FEM model and the known model (Cai et al., 2018) are presented in Fig. 6. It can be observed that the position of the freezing front was underestimated by the model (Cai et al., 2018), while our new model and FEM simulation showed a fair agreement. The temperature distribution is also described by the new model better.

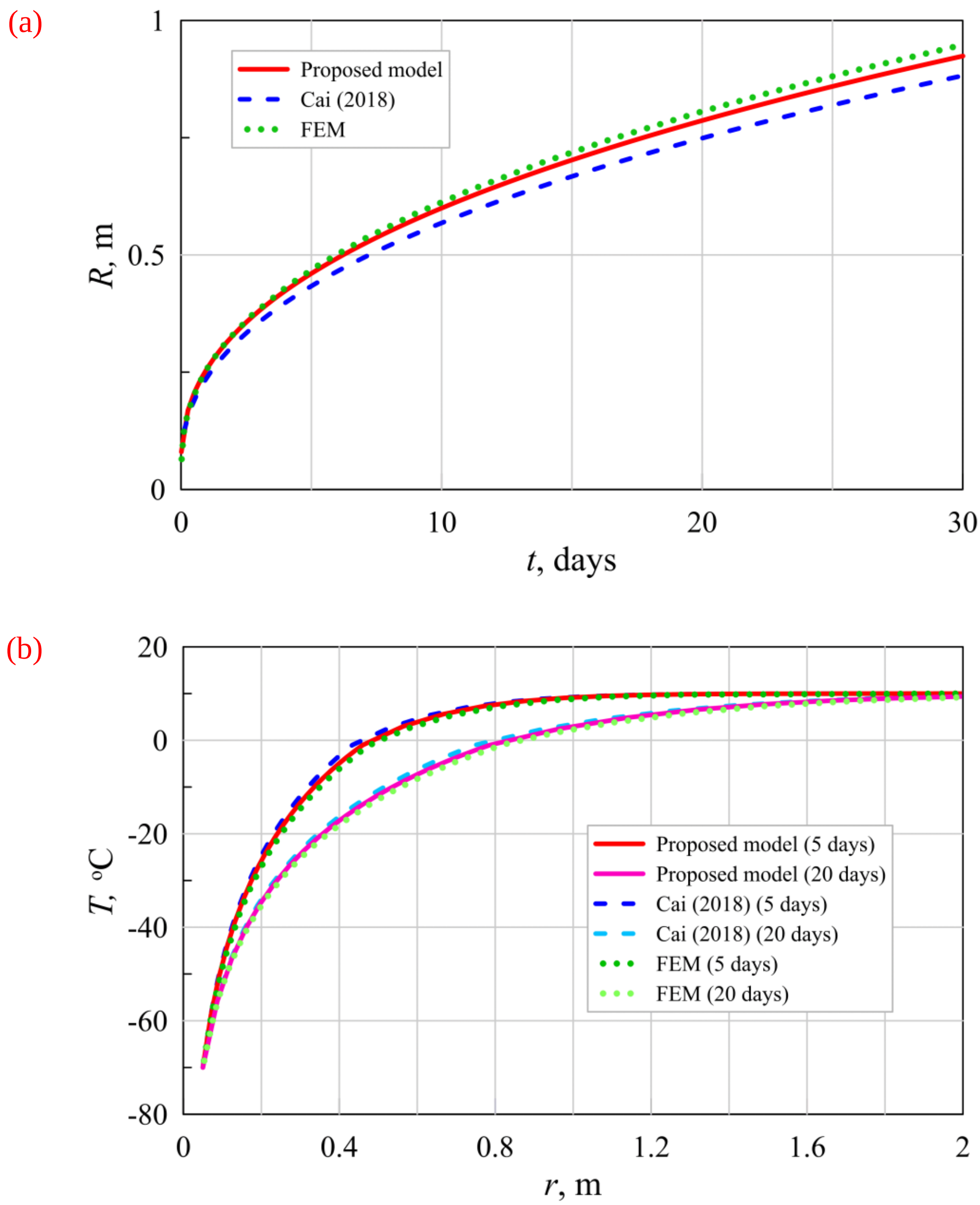

Fig. 6. The position of (a) freezing front and (b) temperature distribution from the proposed semi-analytical solution, the known model (Cai et al., 2018) and FEM simulation.

Based on these results, we can conclude the proposed model of single-ice cylinder formation is very accurate and it can be used for the ground freezing design for the condition of the constant temperature of freeze pipe's wall.

4.2 The formation of plane ice-wall:

For the freezing process using expandable refrigerants, the typical distances between freeze pipes l are normally between 0.8 – 1.2 m, which lets us effectively create the ice-walls with a thickness up to $2l$ (Dorman, 1971). Therefore, in this section, we consider two cases: (Case 1) for the first one the distance between pipes is $l = 1.2$ m and (Case 2) for the second one the distance between pipes is $l = 0.8$ m. For both cases, the thickness of the ice wall, that have to be created, is $2\xi = 2l$.

Based on the developed approach, the proposed problem can be represented as a 1D ice-body close to a wall with constant temperatures, which are defined by Eq. (28), which gives of $\tilde{\tau}_{\mathrm{I}} = -52.5$ °C for $l = 1.2$ m and $\tilde{\tau}_{\mathrm{I}} = -55.9$ °C for $l = 0.8$ m. These values let the coefficient of Eq. (20) from the transcendent equation (19). Fig. 7 compares the results of the semi-analytical model, FEM solution and the known model (Cai et al., 2019, 2018).

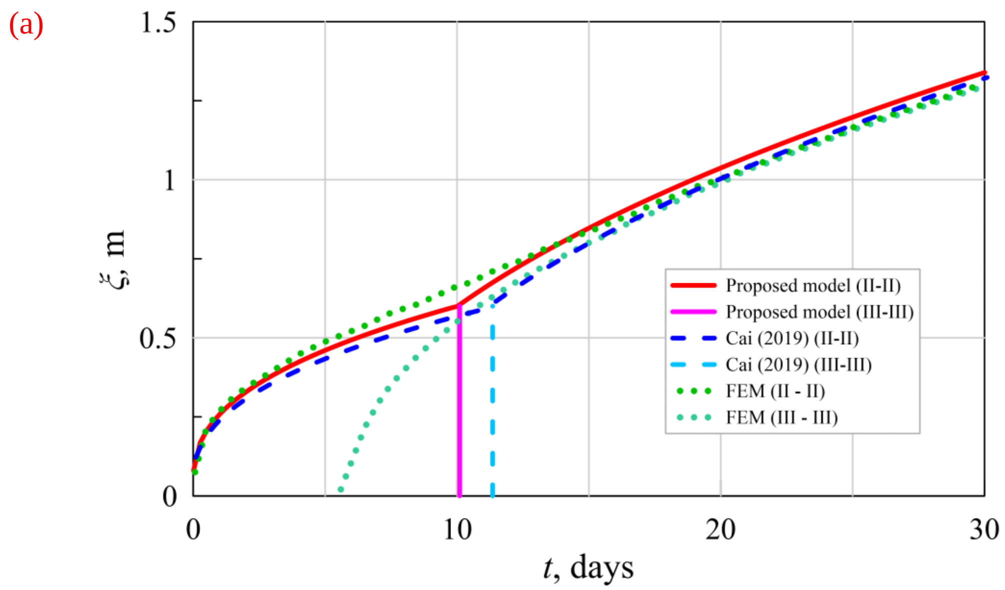

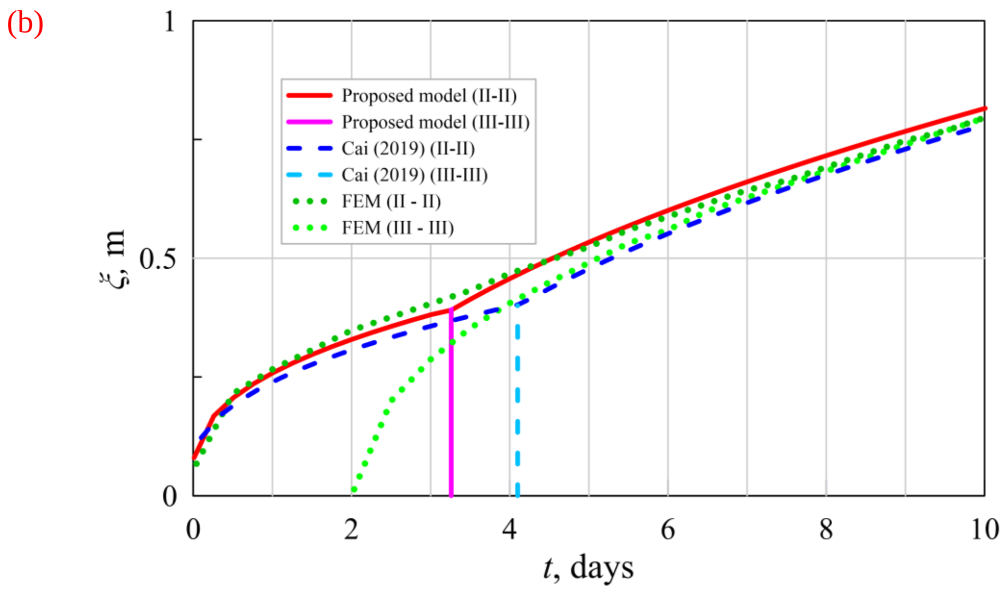

Fig. 7. The position of freezing front based on the relation (20), the model (Cai et al., 2019) and FEM simulation for $l = 1.2$ m(a) and $l = 0.8$ m(b) in cross section II-II and III-III (see Fig. 5)

There is a close agreement between the results of our proposed method with FEM. The overestimation for the thickness of ice-wall after the ice wall closure is less than 10% which is an acceptable range for the ground freezing engineering. The time that is necessary to create the ice wall with the project thickness is predicted well. According to the developed model, the total freezing time to create the ice wall with the thickness $2l$ is 25.2 days for $l = 1.2$ m and 9.8 days for $l = 0.8$ m. For the same condition, the FEM model estimates the freezing time equals 26.5 days for $l = 1.2$ m, and 10.1 days for $l = 0.8$ m. The results indicate that the proposed model is slightly more accurate than the previously developed model (Cai et al., 2019).

5. Validation of the semi-analytical model application to the SCD ground freezing design

To validate the developed model, in this section the results of the analytical model are compared with the results of the laboratory tests that were conducted in 1980th in Moscow Mining Institute and presented in (Shuplik, 1989). During this study, the freezing of saturated soils was performed by a single and a group of 1 m long freeze pipes (0.1 and 0.219 m diameters) that were fulfilled by solid carbon dioxide. The soils were in a thermally insulated box with the sizes of 3.6m x 2.5m x 1m. The pieces of SCD were made by manual crashing of SCD blocks to the sizes of up to 3-4 cm. It should affect the direct application of the results to granulated SCD that is commonly used in practice nowadays, which shape is more uniform and has a small diameter. The thermophysical properties of soil are presented in Table 2. For more details about the experimental methodology and the used automatic measurement equipment, see (Shuplik, 1989).

Table 2. Thermal and physical properties of the soil (Case 2)

Material		Density (kg/m^3)	Thermal conductivity (W/(m°C))	Heat capacity (J/(kg °C))	Latent heat of solidification ($\cdot 10^8$J/m^3)
Coarse grained sand	Frozen	2530	2.7	1420	1.132
	Unfrozen		2.02	1760	

For this case, we do not consider the additional thermal resistance of the freeze pipe wall. The phase transition temperature is 0 °C

5.1 The formation of a single ice cylinder:

Let us make a theoretical assessment of the laboratory results for the freezing of soils by 0.1m and 0.219 m diameter freeze pipes with the soil initial temperatures of 10 °C.

The first step in the application of our semi-analytical model for the formation of a single ice cylinder is to determine the coefficients ω and β_1 (Eq. (14)). It is evident that there is a value of ω at which the parameter β_1 is nearly constant for $t > 3$ days. The function of $\beta_1 = f(\omega, t)$ is considered at two time moments of $t = 3$ days and $t = 50$ days to be able to assume $\omega = 0.431$ and $\beta_1 = 0.247$ for 0.1m diameter and 10 °C initial temperature and $\omega = 0.427$ and $\beta_1 = 0.279$ for 0.219m diameter and 10 °C initial temperature. The position of the freezing front (Eq. (13)) and the results of the laboratory tests (Shuplik, 1989) are presented in Fig. 8.

It can be observed that the position of the freezing front was overestimated by the proposed model during the first 2 days. It is because at the initial period, due to the intense sublimation of SCD the contact between the pipe wall and the refrigerant was not complete, as a result, the temperature of the freeze pipe wall was higher than the constant value used in the model. The disagreement at the final stage of the experiments can be explain by the effects of the boundaries of the soil box that distorted the axisymmetric temperature distribution, whereas the analytical model considers the boundless domain. Nevertheless, the presented agreement can be considered acceptable.

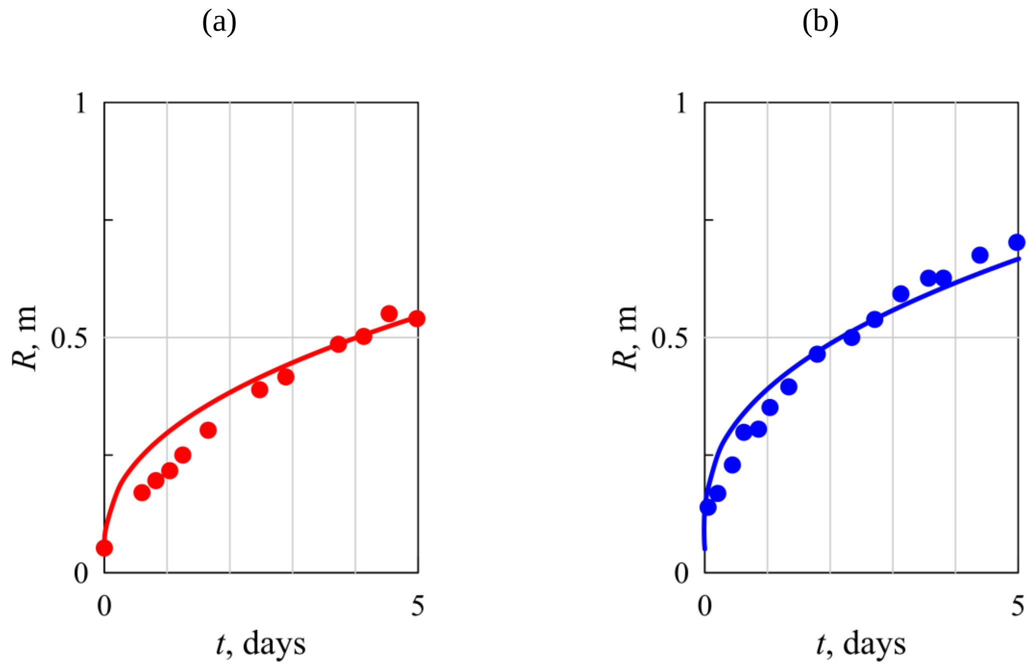

Fig. 8. The position of freezing front from the proposed semi-analytical solution (lines) and the laboratory results (dots) by Shuplik (1989) for the 0.1mdimater freeze pipe (a) and 0.219m diameter freeze pipe (b)

5.2 The formation of plane ice-wall:

In this section, we consider two cases: for the first one, the distance between pipes is $l = 1.1$ m and for the second one, the distance between pipes is $l = 1.5$ m. For both cases, the thickness of the ice wall, that have to be created, is assumed to be $2\xi = 1.2l$.

Based on the developed approach, the proposed problem can be represented as a 1D ice-body close to a wall with constant temperatures, which are defined by Eq. (28), which gives of $\widetilde{\tau}_{\mathrm{I}} = -46.29$ °C for $l = 1.1$ m and $\widetilde{\tau}_{\mathrm{I}} = -40.35$°C for $l = 1.5$ m. These values let the coefficient of Eq. (20) from the transcendent equation (19). Fig. 9 compares the results of the semi-analytical model and the results of the laboratory tests (Shuplik, 1989).

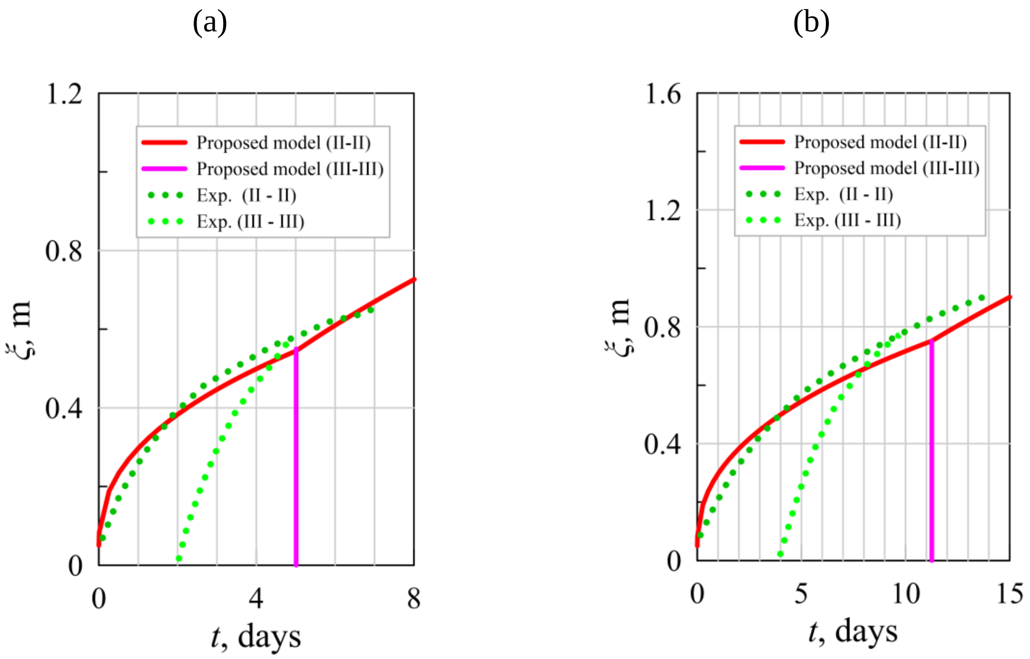

Fig. 9. The position of freezing front based on the relation (20) and laboratory experiment (Shuplik, 1989) for $l = 1.1$ m (a) and $l = 1.5$ m (b) in cross section II-II and III-III (see Fig. 5)

There is a fairly good agreement between the results of the proposed model and the laboratory experiment. The model slightly underestimates the dynamics of the freezing front in the II-II plane for both cases, which can be considered as an additional factor of safety. The time that is necessary to create the ice wall with the project thickness is predicted well. According to the developed model, the total freezing time to create the ice wall with the thickness $1.2l$ is 6.8 days and 7 days based on the semi-analytical model and the experiment respectively for $l = 1.1\, m$; and 15 days and 14 days based on the semi-analytical model and the experiment respectively for $l = 1.5\ m$. Such close agreement can be considered acceptable for engineering practice. It should be noted that, as in the case of a single ice cylinder formation, the disagreement at the final stage of the experiment can be explain by the effects of the boundaries of the consider soil domain, that was used in the laboratory tests, whereas the analytical model is formulated for the boundless domain.

6. Analysis of the influence of additional sources of thermal resistance

The reliability of our developed analytical methods in describing the AGF process with an additional thermal resistance of freeze pipe material and drilling mud is assessed in this section. The soil in the model is medium sand with 35% water content, which properties are applied in accordance with Pimentel et al. (2007). The phase transition temperature is 0 ^{o}C, and the thermophysical properties of drilling mud were calculated based on its density (1290 kg/m^3) and the ratio of clay particles (40wt.%) (Dorman, 1978). The temperature of the freeze pipe is $\tau_0 = -70\ ^{\circ}\mathrm{C}$ as typical conditions for the SCD AGF process. The inner and outer radius of the freeze pipe, as well as the outer radius of the drilling mud layer, are $R_0 = 0.05\ \mathrm{m}$, $R_1 = 0.056\ \mathrm{m}$, and $R_2 = 0.08\ \mathrm{m}$, respectively. Two types of freeze pipe materials were considered as steel and polymer (polyvinyl chloride (PVC)) (Cai et al., 2020). Thermal and physical properties are presented in Table 3 (Eiermann and Hellwege, 1962; Titow, 1984).

Table 3. Thermals and physical properties of the considered materials (Case 3)

Material		**Density (kg/m^3)**	**Thermal conductivity (W/(m ^{o}C))**	**Heat capacity (J/(kg ^{o}C))**	**Latent heat of solidification (10^{-8}J/m^3)**
Polyvinyl chloride		1300	0.16	900	
Steel		7850	50	460	
Drilling mud		1290	1.6	1520	
Sand	Frozen	1958	3.28	2650	1.352
	Unfrozen		2	3850	

6.1 The formation of a single ice cylinder:

The Eq. (14), at two time moments $t = 3$ days and $t = 50$ days, gives $\omega = 0.441$ and $\beta_1 = 0.214$ for a steel (S) freeze pipe and drilling mud (DM) layer, and $\omega = 0.487$ and $\beta_1 = 0.116$ for the polyvinyl chloride (PVC) pipe and DM layer. Without freeze pipe material and DM layer (no W&DM), we have $\omega = 0.418$ and $\beta_1 = 0.256$. As there are not any similar semi-analytical solutions for such a condition, the presented model is only compared with FEM simulation (Fig. 10).

The semi-analytical model defines the dynamic of the ice front with reasonable preciseness. For the PVC pipe, it underestimates the position of ice wall formation compared with FEM up to 9% by the 30 days. It should be noted that the solution without additional sources of thermal resistance may be different for both types of pipe materials. For the case with the steel pipe, the freeze front radius would be up to 7% higher, while the difference could be up to 50% for the case with PVC pipe which indirectly highlights the sensitivity of the AGF simulations to the presence of ice wall material and the drilling mud layer.

(a)

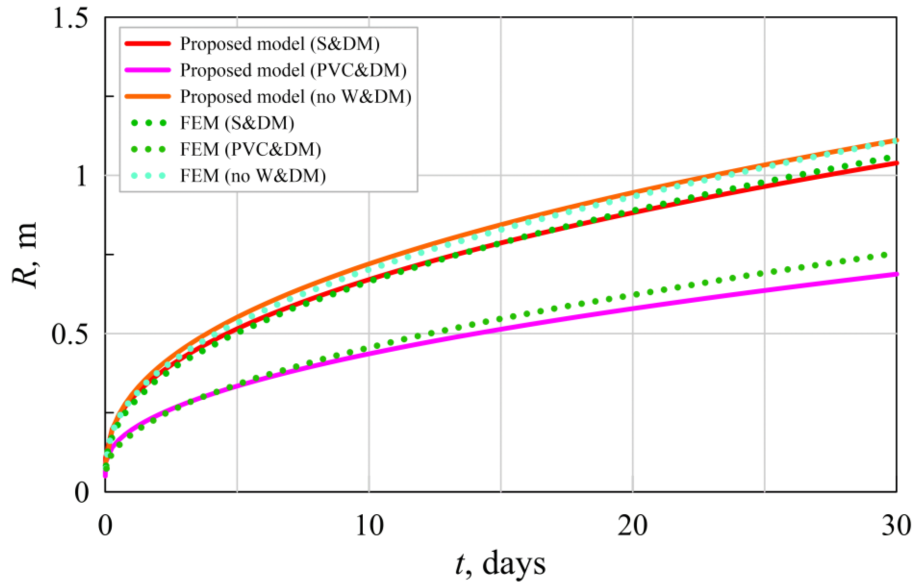

(b)

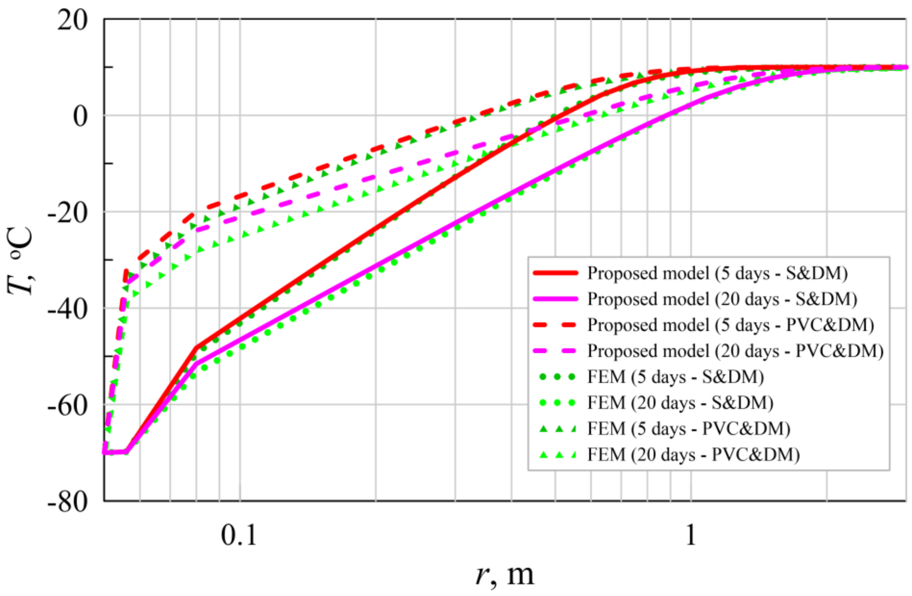

Fig. 10. The position of (a) freezing front and (b) temperature distribution based on the proposed model and FEM simulation.

The presented results demonstrate that the consideration of additional sources of thermal resistance can significantly affect the prediction of single-ice cylinder formation. Even if the difference in the radius with and without the layers of drilling mud and the freeze material may be insufficient, the freezing time is determined completely different. For the present case, the difference in the necessary time for the creation of a 2m diameter ice-cylinder is up to 5 days. For the SCD ground freezing, it means that the refrigerant must de be delivered to the construction site for 5 days more, and the workers who are participating in the loading must also be working for 5 additional days. For example, if the daily consumption of SCD is 50 tonnes/day, it may lead to a shortage of 250 tonnes of refrigerant that very often cannot be replenished without several days of preparation in the SCD production factory.

6.2 The formation of plane ice-wall:

In order to study the behaviour with taking into account the effects of additional sources of thermal resistance, we consider two freeze pipe positions: for the first one the distance between pipes is $l = 1.2$ m and for the second one it is $l = 0.8$ m. For both cases, the project thickness of the ice wall is $2\xi = 2l$. For the case of steel pipes, the constant temperature of the wall was calculated as $\tilde{\tau}_{\mathrm{I}} = -37.8$ °C for $l = 1.2$ m, and $\tilde{\tau}_{\mathrm{I}} = -40.8$ °C for $l = 0.8$ m. These values let the coefficient of Eq. (20) from the transcendent equation (19). The position of the freezing front is presented in Fig. 11.

The analytical and FEM results are in close agreement with regard to the prediction of the freezing front. For ice-wall thickness, the discrepancy between the two solutions is less than 8% during the entire freezing process. The time for reaching the project thickness of the wall is defined fairly accurate by the proposed model. When $l = 1.2$ m, the project thickness is reached on 22.2 days and 22.3 days, according to the developed model and FEM results, respectively. When $l = 0.8$ m, it is reached on 8.7 days and 8.8 days by the same calculation methods.

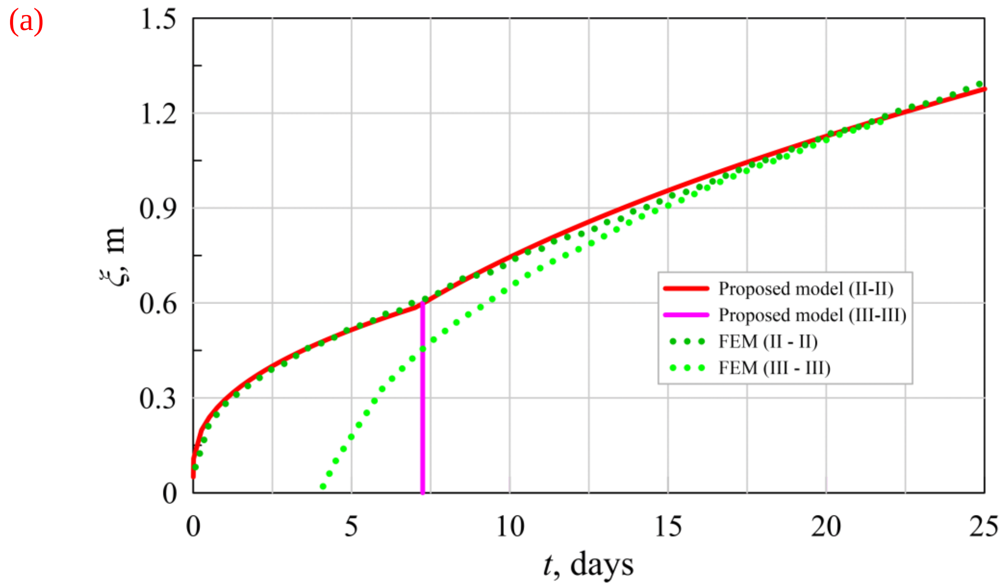

(b)

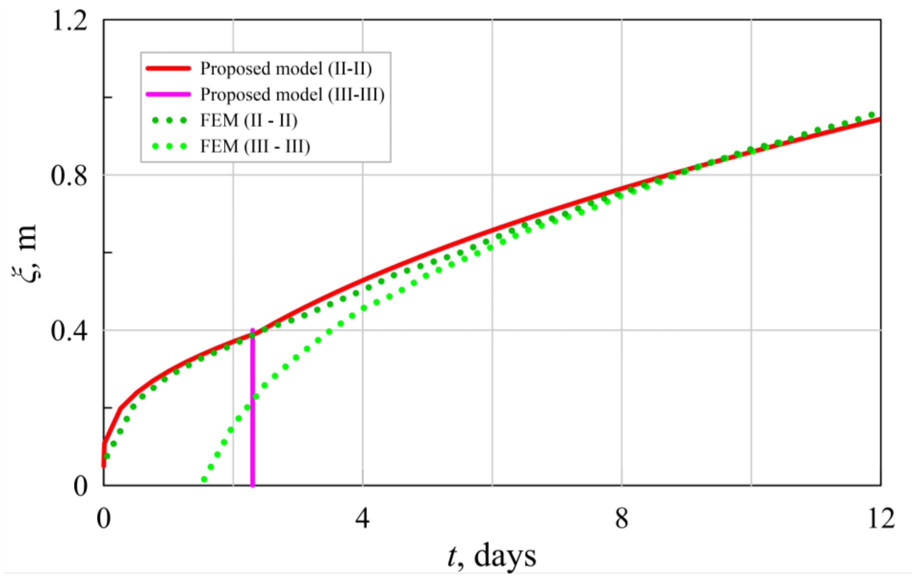

Fig. 11. The position of freezing front for the steel freeze pipe wall based on the relation (20) and FEM simulation for $l = 1.2$ m(a) and $l = 0.8$ m(b) in cross-section II-II and III-III (see Fig. 5)

For the case of PVC pipes, the wall constant temperature is found to be $\widetilde{\tau}_{\mathrm{I}} = -23.9$ °C for $l = 1.2$ m, and $\widetilde{\tau}_{\mathrm{I}} = -24.8$ °C for $l = 0.8$ m based on Eq. (28) which lets us find the coefficient of Eq. (20). The computational results for this semi-analytical model and FEM results are presented in Fig. 12. It is evident that the proposed model does not agree with the simulation results well. However, the inaccurate assessment of the time that is necessary to create the ice wall with the project thickness, may be considered acceptable for engineering purposes. Thus, for $l = 1.2$ m, the project thickness of the ice wall is reached on 44.1 days and 37.2 days, according to the developed model and FEM results, respectively. For $l = 0.8$ m, it is reached on 18.0 days and 15.2 days by the same calculation methods. The discrepancies are less than 18%. As in both cases, the developed model overestimates the time of freezing, this difference may be considered as an additional safety factor.

It should be noted that even if the developed semi-analytical model can describe the dynamic of single ice cylinder formation for the PVC freeze pipe quite well (see Section 6.1), in the case of the group of freeze pipes, the model accuracy during the first stage of ice wall formation is worse. It happens because, for the PVC pipes, the time of the first stage is sufficiently longer than for the steel pipe, due to that the influence of the neighbouring pipes became sufficient. In this case, the initial assumption that the process of the ice-wall formation can be divided into two independent stages became less accurate. More detailed mathematical representation of the first stage of ice wall formation can significantly improve the overall accuracy of the model, as even now, the second stage is described qualitatively well.

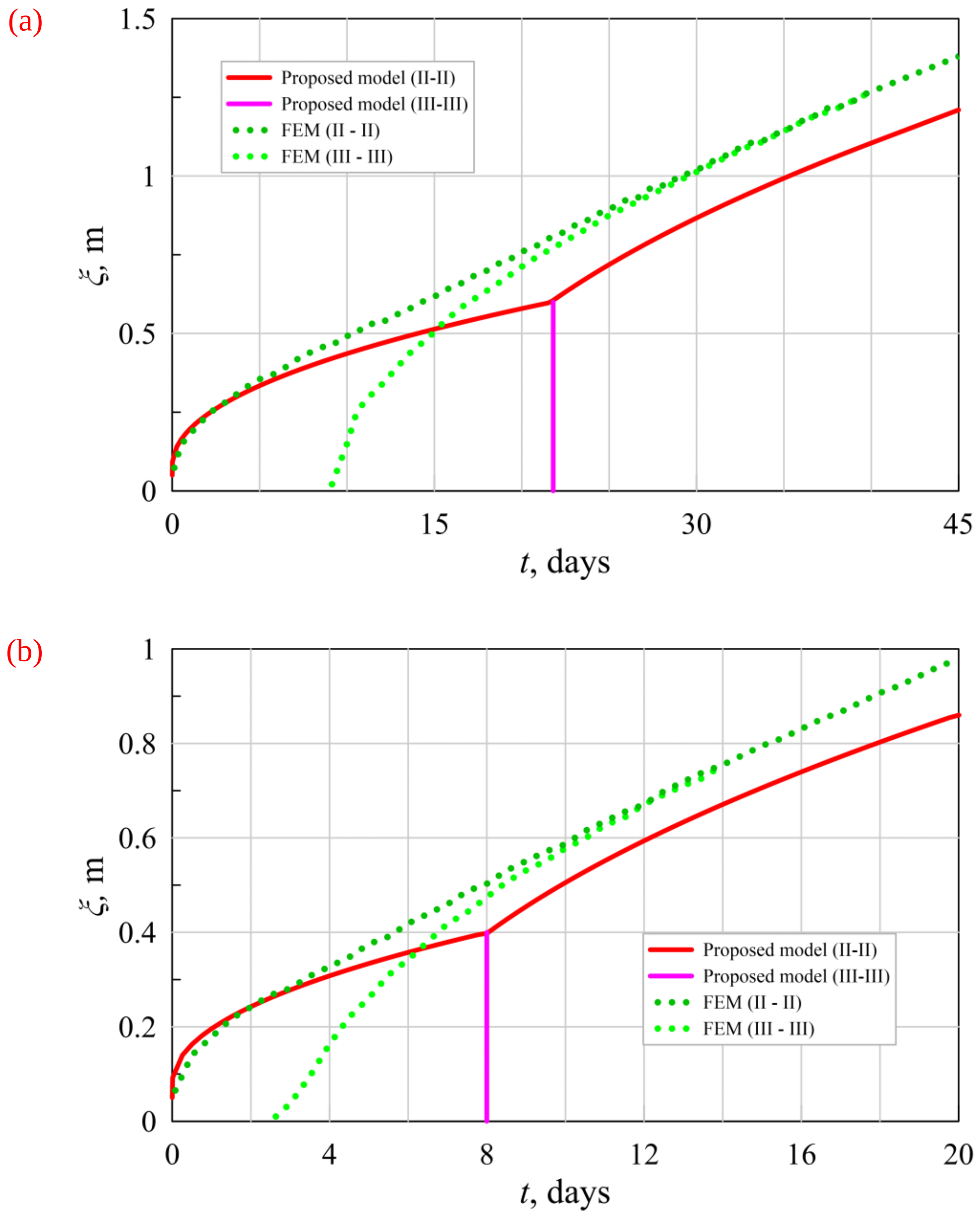

Fig. 12. The position of freezing front for the PVC freeze pipe wall based on the relation

(26), and FEM simulation for $l = 1.2$ m(a) and $l = 0.8$ m(b) in cross-section II-II and III-III (see Fig. 5)

The proposed model is the first sufficiently accurate semi-empirical model that lets us consider additional sources of thermal resistance during AGF design. This section provided a further demonstration that the additional sources of thermal resistance should be considered during the AGF design to ensure the accurate determination of freezing time and, based on it, the accurate schedule for the solid carbon dioxide delivery to the construction site.

In the next section, we will consider the ability of the developed model to determine the solid carbon dioxide consumption rate.

7. Determination of solid carbon dioxide consumption

To illustrate the ability of the developed model to determine solid carbon dioxide consumption, let us define this parameter for the conditions of the examples discussed in the previous sections.

The consumption of SCD was calculated at any time by Eq. (32) (a pipe with $h = 1$ m) and compared with FEM as shown in Fig. 13a. The presented results demonstrate that the difference between FEM and the semi-analytical solution is less than 11% for both freeze pipe materials. In Fig. 13b, the comparison between the results of the semi-analytical model and the laboratory experiment is presented for the case of 0.1m diameter freeze pipe. This experiment was conducted twice. Even if the semi-analytical model slightly underestimates the consumption of SCD during the initial period, the overall agreement can be considered very good. Therefore, the proposed model can effectively be used to determine the solid carbon dioxide consumption rate during the formation of single ice cylinders.

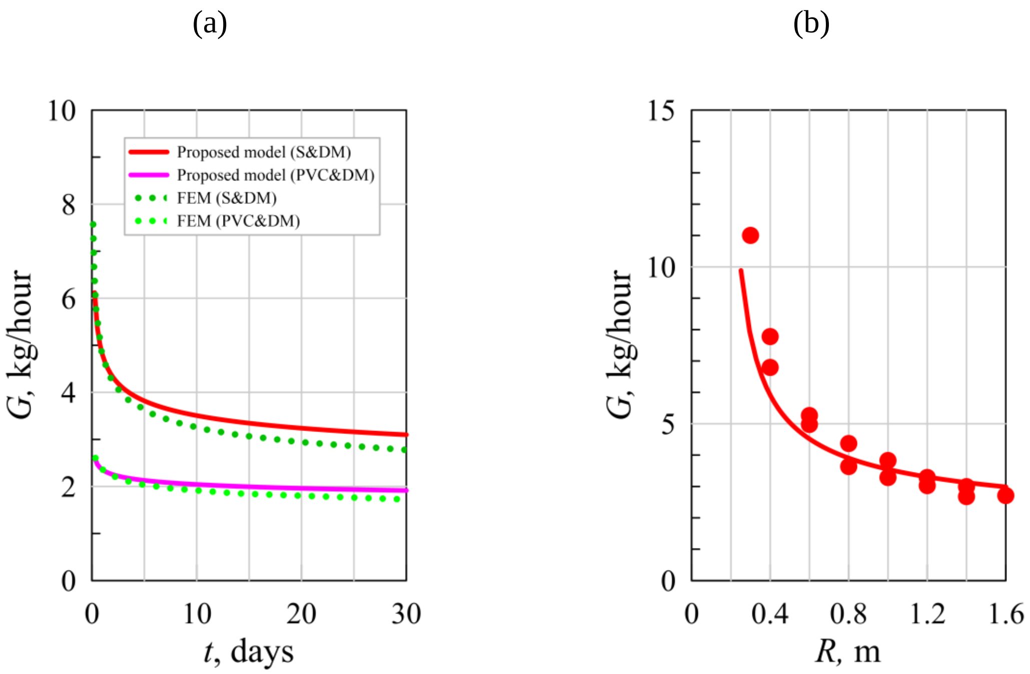

Fig.13. The consumption of SCD during the formation of a single ice-cylinder according to the relation (32) and FEM simulation (a), and according to the relation (38) and the laboratory experiment by Shuplik (1989) (b).

At any time for the pipes with the length of $h = 1$ m, from Eq. (32) and (33), a similar rate can be calculated from the proposed model and FEM simulation as shown in Fig. 14.

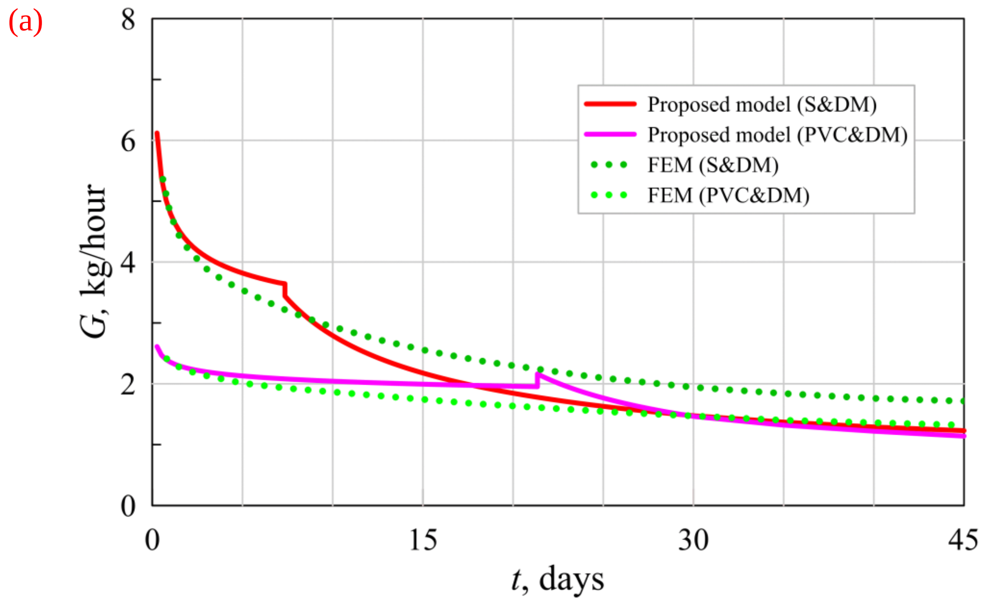

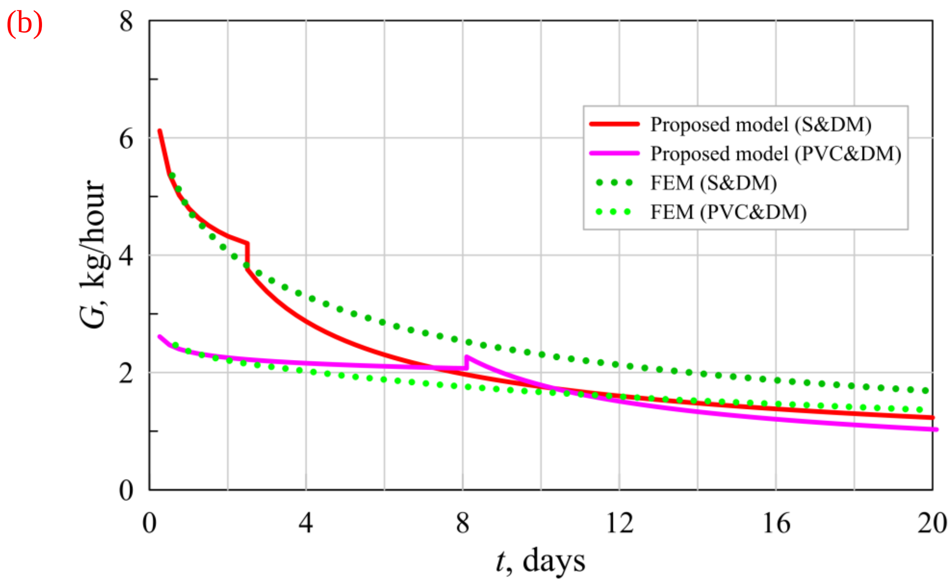

Fig. 14. The consumption of SCD during the formation of plane ice-wall according to the relations (32) and (33) and FEM simulation, a – for 1.2 m, b – 0.8 m

The results show that the proposed relation (32) overestimates the consumption of SCD until the moment when separate ice cylinders are merged. In addition, the calculated results by the relation (33) are smaller than the simulation results. The difference observed can be up to 30%. This fact illustrates the limitations of the proposed semi-analytical model for the assessment of refrigerant consumption. A more accurate approach for the determination of the average temperature in the I-I plane can increase the preciseness of the presented model, however, it is still under development.

8 Conclusions

This paper introduced a new semi-analytical model for the artificial ground freezing by using solid carbon dioxide process which describes the dynamics of single ice cylinders formation and(b) resultant plane ice wall development where separate cylinders are being merged. The model is developed to assume a constant temperature on the inner freeze pipe's surface (e.g., Dirichlet boundary condition). For the first time, our analytical model considers additional sources of thermal resistances (freeze pipe materials, drilling mud and casting pipe walls) in the calculation of AGF dynamic parameters and also determines the consumption of solid carbon dioxide during the formation of the ice wall. The dynamic parameters of the AGF process predicted by our model are more accurate than those of the available models when compared with numerical simulation. For the typical freezing conditions, the discrepancy between the results of our model and FEM results for the prediction of the freezing time to create the ice wall with the project thickness is less than 4% for the steel pipes and 18% for polyvinylchloride freeze pipes. The proposed model provides fairly accurate results and can be used to design artificial ground freezing by using solid carbon dioxide for engineering practices and generalised for the construction of thermal energy systems.

To develop a further understanding of the ice wall formation that is delivered by solid carbon dioxide ground freezing, the following questions should be answered in the future studies:

1. How does heat transfer to the freeze pipes fulfilled by solid carbon dioxide is changing over the depth?
2. How do properties of SCD (density, grain shape and size etc.) affect the intensity of heat transfer?
3. Which loading regime of the solid carbon dioxide granules should be maintained to ensure the economically effective formation of the ice wall?
4. How can the application of the SCD ground freezing change the frost heave behaviour of frozen soils?
5. Which polymer material is the most suitable for the freeze pipes? What is the optimum application range for such types of freeze pipes?

Acknowledgements

Petr Nikolaev would like to thank Prof. Mikhail Shuplik who is one of the founders of this ground freezing method and who devoted more than 30 years to its development and

introduction to many geotechnical projects; Prof. Shuplik was his supervisor for many years and introduced to him this unique ground freezing method and inspired him to develop this research.

References

Alzoubi, M.A., Xu, M., Hassani, F.P., Poncet, S., Sasmito, A.P., 2020. Artificial ground freezing: A review of thermal and hydraulic aspects. Tunnelling and Underground Space Technology 104, 103534. https://doi.org/10.1016/j.tust.2020.103534

Andersland, O.B., Ladanyi, Branko., ASCE, 2004. Frozen Ground Engineering, 2nd Edition. Wiley.

Bakholdin, B. V., 1963. The choice of the optimal regime of artificial ground freezing for construction purposes (in Russian). Gosstroyizdat, Moscow.

Bell, F.G., 2013. Methods of Treatment of Unstable Ground., Methods of Treat of Unstable Ground. Elsevier.

Boles, M.A., Ozisik, M.N., 1983. Exact Solution for Freezing in Cylindrically Symmetric, Porous, Moist Media. Journal of Heat Transfer 105, 401–403. https://doi.org/10.1115/1.3245593

Cai, H., Li, P., Wu, Z., 2020. Model Test of Liquid Nitrogen Freezing-Temperature Field of Improved Plastic Freezing Pipe. Journal of Cold Regions Engineering 34, 4020001. https://doi.org/10.1061/(ASCE)CR.1943-5495.0000204

Cai, H., Liu, Z., Li, S., Zheng, T., 2019. Improved analytical prediction of ground frost heave during tunnel construction using artificial ground freezing technique. Tunnelling and Underground Space Technology 92, 103050. https://doi.org/10.1016/j.tust.2019.103050

Cai, H., Xu, L., Yang, Y., Li, L., 2018. Analytical solution and numerical simulation of the liquid nitrogen freezing-temperature field of a single pipe. AIP Advances 8, 055119. https://doi.org/10.1063/1.5030442

Charny, N.A., 1948. Underground Hydromechanics. Gostehteorizdat.

Davydov, V.V., 1980. Handbook on the construction of mine shafts by ground improvment methods (in Russian). Nedra, Moscow.

Dorman, Ya.A., 1978. VSN 189-78 Instructions for the design and production of works on artificial ground freezing during the construction of subways and tunnels. Mintransstry, Moscow.

Dorman, Ya.A., 1971. Artificial ground freezing during construction of underground railway systems (in Russian). Transport, Moscow.

Eiermann, K., Hellwege, K.H., 1962. Thermal conductivity of high polymers from −180°C. to 90°C. Journal of Polymer Science 57, 99–106. https://doi.org/10.1002/pol.1962.1205716508

Harris, J.S., 1995. Ground freezing in practice. Ground freezing in practice. https://doi.org/10.1016/s0165-232x(96)00008-0

Hu, J., Liu, Y., Wei, H., Yao, K., Wang, W., 2017. Finite-element analysis of heat transfer of horizontal ground-freezing method in shield-driven tunneling. International Journal of Geomechanics 17, 4017080. https://doi.org/10.1061/(ASCE)GM.1943-5622.0000978

Hu, R., Liu, Q., 2016. Simulation of heat transfer during artificial ground freezing combined with groundwater flow, in: 2016 COMSOL Conference in Munich. pp. 2–7.

Hu, R., Liu, Q., Xing, Y., 2018. Case Study of Heat Transfer during Artificial Ground Freezing with Groundwater Flow. Water 10, 1322. https://doi.org/10.3390/w10101322

Hu, X., Han, L., Han, Y., 2019. Analytical solution to temperature distribution of frozen soil wall by multi-row-piped freezing with the boundary separation method. Applied Thermal Engineering 149, 702–711. https://doi.org/10.1016/j.applthermaleng.2018.12.096

Hu, X., Yu, J., Ren, H., Wang, Y., Wang, J., 2017. Analytical solution to steady-state temperature field for straight-row-piped freezing based on superposition of thermal potential. Applied Thermal Engineering 111, 223–231. https://doi.org/10.1016/j.applthermaleng.2016.09.058

Huang, S., Guo, Y., Liu, Y., Ke, L., Liu, G., Chen, C., 2018. Study on the influence of water flow on temperature around freeze pipes and its distribution optimization during artificial ground freezing. Applied Thermal Engineering 135, 435–445. https://doi.org/10.1016/j.applthermaleng.2018.02.090

Huang, X., Rudolph, D.L., 2022. A hybrid analytical-numerical technique for solving soil temperature during the freezing process. Advances in Water Resources 162, 104163. https://doi.org/10.1016/j.advwatres.2022.104163

Jiang, B.S., Shen, C.R., Feng, Q., 2010. Analytical formulation of temperature field of single freezing pipe with constant outer surface temperature. Meitan Xuebao/Journal of the China Coal Society 35, 923–927.

Kakaç, S., Yener, Y., Naveira-Cotta, C.P., 2018. Heat Conduction, 5th ed. CRC Press.

Li, T., Zhou, Y., Shi, X., Hu, X., Zhou, G., 2018. Analytical solution for the soil freezing process induced by an infinite line sink. International Journal of Thermal Sciences 127, 232–241. https://doi.org/10.1016/j.ijthermalsci.2018.01.013

Lunardini, V.J., Varotta, R., 1981. Approximate Solution to Neumann Problem for Soil Systems. Journal of Energy Resources Technology 103, 76–81. https://doi.org/10.1115/1.3230817

Maksimov, G.N., Zamyatin, S.I., 1969. The experience of carbon dioxide cooling of basement soils under a prefabricated building in the southern distribution zone of permafrost soils (in Russia), in: Proceedings of the All-Union Scientific and Technical Meeting on Improving Large-Panel Building Construction in Areas of Permafrost and Harsh Climate. Moscow, pp. 37–90.

Nikolaev, P., Sedighi, M., Jivkov, A.P., Margetts, L., 2022. Analysis of heat transfer and water flow with phase change in saturated porous media by bond-based peridynamics. International Journal of Heat and Mass Transfer 185, 122327. https://doi.org/10.1016/j.ijheatmasstransfer.2021.122327

Nikolaev, P., Shuplik, M., 2019. Low-temperature ground freezing methods for underground construction in urban areas. MATEC Web of Conferences 265, 04020. https://doi.org/10.1051/matecconf/201926504020

Nikolaev, P.V., 2016. Investigation of the Regimes of Solid Carbon Dioxide Ground Freezing in Underground Construction (in Russian). Cand. of Eng. Sc. Thesis. National University of Science and Technology MISIS.

Pimentel, E., Sres, A., Anagnostou, G., 2007. Modelling of ground freezing in tunnelling. “Proceedings of the 33rd ITA-AITES World Tunnel Congress - Underground Space - The 4th Dimension of Metropolises” 1, 331–336. https://doi.org/10.1201/noe0415408073.ch56

Shao, Z., Hu, X., Han, Y., Fang, T., 2020. Generalized analytical solution to steady-state temperature field of double-circle-piped freezing. Cold Regions Science and Technology 175, 103076. https://doi.org/10.1016/j.coldregions.2020.103076

Shuplik, M., Nikolaev, P., 2019. Advanced ground freezing method and its applications in underground construction. MATEC Web of Conferences 265, 04021. https://doi.org/10.1051/matecconf/201926504021

Shuplik, M.N., 1989. Justification and development of resource-saving technologies for ground freezing during the construction of urban underground structures (in Russian). Dr. of Eng. Sc. Thesis. Moscow Mining Institute.

Shuplik, M.N., Nikitushkin, R.A., 2011. Estimation of temperature losses during ground freezing by horizontal freeze pipe (in Russian). Mining Informational and analytical bulletin 2, 138–142.

Shuster, J.A., 1972. Controlled freezing for temporary ground support, in: Proceedings of the First Rapid Excavation and Tunneling Conference. AIME, Chicago, pp. 863–895.

Titow, W. V., 1984. PVC Technology, PVC Technology. Springer Science & Business Media. https://doi.org/10.1007/978-94-009-5614-8

Tounsi, H., Rouabhi, A., Tijani, M., Guérin, F., 2019. Thermo-Hydro-Mechanical Modeling of Artificial Ground Freezing: Application in Mining Engineering. Rock Mechanics and Rock Engineering 52, 3889–3907. https://doi.org/10.1007/s00603-019-01786-9

Trupak, N.G., 1974. Artificial ground freezing in underground construction work (in Russian). Nedra, Moscow.

Xu, M., Akhtar, S., Zueter, A.F., Auger, V., Alzoubi, M.A., Sasmito, A.P., 2020. Development of Analytical Solution for a Two-Phase Stefan Problem in Artificial Ground Freezing Using Singular Perturbation Theory. Journal of Heat Transfer 142. https://doi.org/10.1115/1.4048137

Zhou, Y., Hu, X., Li, T., Zhang, D., Zhou, G., 2018. Similarity type of general solution for one-dimensional heat conduction in the cylindrical coordinate. International Journal of Heat and Mass Transfer 119, 542–550. https://doi.org/10.1016/j.ijheatmasstransfer.2017.11.131

Zhou, Y., Zhou, G.Q., 2012. Analytical solution for temperature field around a single freezing pipe considering unfrozen water. Meitan Xuebao/Journal of the China Coal Society 37, 1649–1653.

Zueter, A., Nie-Rouquette, A., Alzoubi, M.A., Sasmito, A.P., 2020. Thermal and hydraulic analysis of selective artificial ground freezing using air insulation: Experiment and modeling. Computers and Geotechnics 120, 103416. https://doi.org/10.1016/j.compgeo.2019.103416

Zueter, A.F., Xu, M., Alzoubi, M.A., Sasmito, A.P., 2021. Development of conjugate reduced-order models for selective artificial ground freezing: Thermal and computational analysis. Applied Thermal Engineering 190, 116782. https://doi.org/10.1016/j.applthermaleng.2021.116782